ISSN No:-2456-2165

Analysis and Design of Air Intake of Scramjet Engine for Lower Starting Mach Number

Vatsal Sorathia
Defence Institute of Advance Technology.
Pune(411023), India

Abstract:- This paper proposes an analysis and design of air intake of scramjet engine for lower starting Mach number at M=3.5. In the current scenario, there are lots of researches have been carried out towards the vehicle with a combined propulsion system for getting high performance and efficiency while pursuing a very wide range of operating Mach number. Due to various propulsion systems, weight reduction is a very challenging task for this type of vehicle. So if we can somehow reduce the starting Mach number of scramjet engine then we can reduce the required propulsion system, as the bridge between the maximum possible velocity of the low-speed engine and the scramjet start velocity. In beginning, the basic geometry of hypersonic intake with shock structure is given followed by the theoretical equations of various design parameters at various sections of the scramjet engine. Next, various geometries of intake are constructed with a combination of a different number of ramps and with different ramp angles. Analysis of intake geometries against lower Mach number flow is carried out by CFD simulations and various flow parameters are measured. From these flow parameters, performance parameters are found and compare various intake geometries based on them.

Keywords:- Lower starting Mach number, Hypersonic, Scramjet, Air-intake, Ramp angle, CFD.

Nomenclature

T= Static temperature
P= Static pressure
V= Velocity
ρ = Density
R=Gas constant
C_p=Specific heat
A=Area
f= Fuel to air ratio
f_{st}= Stoichiometric fuel to air ratio
M= Mach number
γ= Ratio of specific heats
$\emptyset$= Equivalence ratio
S= Specific fuel consumption
$\frac{V_{fx}}{V_3}$ =Ratio of Fuel Injection Axial Velocity To Combustor Entrance Velocity

$\frac{V_f}{V_3}$ =Ratio of Fuel Injection Total Velocity to Combustor Entrance Velocity

$C_f \frac{A_w}{A_3}$ =Burner Effective Drag Coefficient

h_{PR} = Heat of reaction

h_f =Absolute Sensible Enthalpy of Fuel Entering Combustor

IT= Ignition temperature

T^0 = Reference temperature

η_{th} = Thermal Efficiency

η_p =Propulsive Efficiency

η_c = Inlet Compression System Efficiency
$\eta_{b=}$Burner Efficiency

η_e = Expansion System Efficiency

C_{p0} =Specific Heat of Freestream Air

C_{pc} =Specific Heat for Engine Compression

C_{pb} =Specific Heat for Engine Burner

C_{pe} =Specific Heat for Engine Expansion

γ_c= Ratio of Specific Heats for Compression

γ_b= Ratio of Specific Heats for Burner

γ_e= Ratio of Specific Heats for Expansion

θ = Ramp angel

β = Oblique shock angel

$\frac{F}{\dot{m}_0}$ = Specific thrust

g= Gravity

ISSN No:-2456-2165

I. INTRODUCTION

In this era of missile propulsion, there are several types of research are going on scramjet engine technology. It is the most complex propulsion system in all and there are many challenges in the development of the scramjet engine and its application, which I described in the following discussion. The scramjet engine is the air-breathing engine and it is working efficiently only at design Mach number while there are no moving parts in the compression system. In off-design conditions, it cannot work with its highest efficiency and sometimes the engine cannot even start. So now if we talk about the development of some vehicle, which we want to operate in a large operating Mach number range then we must need more than one propulsion system. Every propulsion has its own efficient Mach number range in which it can work in an efficient manner. Figure (1.1.1) [2]. given below displays a chart of propulsion systems and their suitable Mach number range. So from this graph, we can easily get the point that for operating in a wider range efficiently, then we must include all the required propulsion systems.

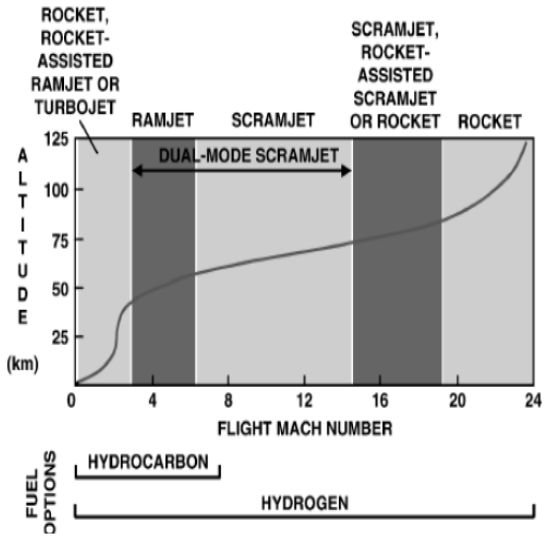

Fig. 1.1.1: Operating Mach number range of different propulsion systems [2] .

So when a vehicle has more than one propulsion system, the total weight of the vehicle goes very high. So for getting efficient operation we must take care about weight reduction. When all the propulsion systems are required, at that time weight reduction is a very challenging task for the development of this type of hybrid vehicle. In addition to this, without weight reduction, we cannot get good payload carrying capacity up to some realistic limit. If somehow we can reduce the scramjet starting Mach number then we can reduce the number of required propulsion systems, as the gap is fill between the maximum possible velocity of the low-speed engine and the scramjet start velocity. So this will ultimately get overall vehicle weight reduction and achieve more payload capacity.

1.2 Scramjet Theory

The equations of different flow parameters at the various designation shown in fig(1.2.1) are given below and directly taken from [12]:

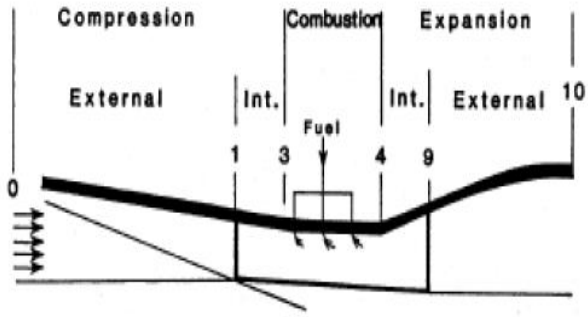

Fig. 1.2.1: Scramjet reference station designation [12].

$$M_3 = \sqrt{\frac{2}{\gamma_c - 1}\left\{\frac{T_0}{T_3}\left(1 + \frac{\gamma_c - 1}{2} M_0^2\right) - 1\right\}} \quad (1)$$

Compression Component (0-3):

- Stream thrust function at free stream conditions:

$$Sa_0 = V_0\left(1 + \frac{RT_0}{V_0^2}\right) \quad (2)$$

- Combustor entrance temperature

$$T_3 = \emptyset T_0 \quad (3)$$

- Combustor entrance velocity

$$V_3 = \sqrt{V_0^2 - 2C_{pc}T_0(\emptyset - 1)} \quad (4)$$

- Stream thrust function at combustor entrance

$$Sa_3 = V_3\left(1 + \frac{RT_3}{V_3^2}\right) \quad (5)$$

- Ratio of combustor entrance pressure to free stream pressure

$$\frac{P_3}{P_0} = \left\{\frac{\emptyset}{\emptyset(1-\eta_c)+\eta_c}\right\}^{\frac{Cpc}{R}} \quad (6)$$

- Ratio of combustor entrance are to free stream entrance area

$$\frac{A_3}{A_0} = \emptyset \frac{P_0}{P_3}\frac{V_0}{V_3} \quad (7)$$

Combustion Components (3-4):

- Combustor exit velocity

$$V_4 = V_3\left\{\frac{1+f\frac{V_{fx}}{V_3}}{1+f} - \frac{C_f\frac{A_w}{A_3}}{2(1+f)}\right\} \quad (8)$$

- Combustor exit temperature

$$T_4 = \frac{T_3}{1+f}\left\{1 + \frac{1}{C_{pb}T_3}\left[\eta_b f h_{PR} + f h_f + f C_{pb} T^0 + \left(1 + f\frac{V_f^2}{V_3^2}\right)\frac{V_3^2}{2}\right]\right\} - \frac{V_4^2}{2C_{pb}} \quad (9)$$

- Ratio of area at combustor exit to combustor entrance

$$\frac{A_4}{A_3} = (1+f)\frac{T_4}{T_3}\frac{V_3}{V_4} \quad (10)$$

- Stream thrust function at combustor exit conditions

$$Sa_4 = V_4\left(1 + \frac{RT_4}{V_4^2}\right) \quad (11)$$

Expansion Components (4-10):

- Temperature at engine exit

$$T_{10} = T_4\left\{1 - \eta_e\left[1 - \left(\frac{P_{10}}{P_0}\frac{P_0}{P_4}\right)^{\frac{R}{Cpe}}\right]\right\} \quad (12)$$

- Velocity at engine exit

$$V_{10} = \sqrt{V_4^2 + 2C_{pe}(T_4 - T_{10})} \quad (13)$$

- Stream thrust function at engine exit condition

$$Sa_{10} = V_{10}\left(1 + \frac{RT_{10}}{V_{10}^2}\right) \quad (14)$$

- Ratio of area at engine exit to area at free stream entrance

$$\frac{A_{10}}{A_0} = (1+f)\frac{P_0}{P_{10}}\frac{T_{10}}{T_0}\frac{V_0}{V_{10}} \quad (15)$$

Overall Engine Performance Measures

- Specific thrust

$$\frac{F}{\dot{m}_0} = (1+f)Sa_{10} - Sa_0 - \frac{RT_0}{V_0}\left(\frac{A_{10}}{A_0} - 1\right) \quad (16)$$

- Specific fuel consumption

$$S = \frac{f}{\frac{F}{\dot{m}_0}} \quad (17)$$

- Specific impulse

$$I_{sp} = \left(\frac{h_{PR}}{g_0 V_0}\right)\eta_0 \quad (18)$$

- Overall efficiency

$$\eta_0 = \frac{V_0}{h_{PR}S} \quad (19)$$

- Thermal efficiency

$$\eta_{th} = \frac{\left[(1+f)\frac{V_{10}^2}{2}\right] - \frac{V_0^2}{2}}{f h_{PR}} \quad (20)$$

- Propulsive efficiency

$$\eta_P = \frac{\eta_0}{\eta_{th}} \quad (21)$$

For getting successful combustion in combustor, air entered in combustor must has a temperature higher than an ignition temperature of corresponding fuel. Ignition temperature of fuel is defined as a temperature at which fuel has no need to any spark for getting ignite. IT of fuel is very important thing in our project because at moment of starting of scramjet engine, air flow entered in intake has very low speed of Mach 3.5, so it will has relatively low temperature at intake of combustor. Ignition temperature of various fuels are given below and taken from [13, 14, 15] :

Fuel	IT (K)
Hydrogen	845.15
Methane	810.15
Ethane	745.15
JP-10	518.15
JP-7	514.15
Hexane	498.15
Octane	479.15

Scramjet engine is nothing but the supersonic combustion ramjet. So after combustion of fuel, burned gases must have speed higher than Mach 1 at end of combustor in case of scramjet engine. As we seen in equations given above, combustor exit velocity is highly depend on combustor entry velocity i.e. V_3 and fuel-to-air ratio (f). combustor exit temperature is depend on combustor entry temperature (T_3), combustor entry velocity (V_3), fuel-to-air ratio (f), combustor ext velocity (V_4) and heat of reaction of fuel. Here parameters V_3 & T_3 we can control by proper intake design. So ultimately, Mach No. at combustor exit (M_4) is depend on intake design as well as fuel-to-air ratio (f) and heat of reaction of fuel(hPR). Kristen Roberts [12] has shown effect of fuel-to-air ratio (f) on combustor exit Mach No(M_4). He showed that as we decrease the value of fuel-to-air ratio (f) from value stoichiometric fuel-to-air ratio (f_{st}) of corresponding fuel, combustor exit Mach No(M_4) will goes to increase.

stoichiometric fuel-to-air ratio (f_{st}) of various fuels are given below and calculated from (22) taken from [12] :

$f_{st} = \frac{36x+3y}{103(4x+y)}$ where the fuel s represented in the form of C_xH_y (22)

Table 1: Stoichiometric fuel-to-air ratio (f_{st}) of various listed fuels

Fuel Type	Chemical Formula	f_{st}
Hydrogen	H_2	0.0291
Methane	CH_4	0.0583
Ethane	C_2H_6	0.0624
JP-10	$C_{10}H_{16}$	0.0707
JP-7	$C_{12}H_{25}$	0.0674
Hexane	C_6H_{14}	0.0659
Octane	C_8H_{18}	0.0664

There is some limit for variation in fuel-to-air ratio, equivalence ratio (∅) is used as a limiting parameter for that. Equivalence ratio is defined as a ratio of fuel-to-air ratio used (f) to the stoichiometric fuel-to-air ratio (f_{st}) .

$$\because \emptyset = \frac{f}{f_{st}} \quad (23)$$

Heiser and pratt [12] stats that a general guidelines for the equivalence ratio is from 0.2 to 2 for "combustion to occur within a useful timescale."

Heats of reaction of corresponding fuels per mass are given below and taken from [1, 16, 17]

Table 2: Heat of reaction of various listed fuels.

Fuel Type	$h_{PR}\left(\frac{KJ}{Kg\ Fuel}\right)$
Hydrogen	119954
Methane	50010
Ethane	47484
JP-10	42100
JP-7	43903
Hexane	45100
Octane	44786

As we have seen in the equations given above, the whole performance of the scramjet engine is dependent on the performance of the inlet. The performance of the engine depends on how efficiently can inlet compress the intake air and how much pressure recovery the intake can achieve. Compression and pressure recovery of intake air depend on the structure of oblique shocks, which directly depend on the configuration of the inlet such as the number of ramps present in the inlet and angles between each pair of adjacent ramps. So proper design of inlet according to an application would give an expected performance of the scramjet engine.

1.3 One- Dimensional Flow Analysis

1.3.1 Oblique Shock Wave Relations

As we discussed, in hypersonic intake, air is compressed by multiple oblique shock waves. So for getting idea about various flow parameters at the end of intake and shock deflection angle at every ramp, oblique shock wave relations are used for this purpose. Flow properties at downward side of oblique shock wave are calculated by flow properties at upward side and flow turning angle [3].

First, relation between M-θ-β is given by (24) [3]:

$$tan\theta = 2cot\beta \frac{M_1^2 \sin^2\beta - 1}{M_1^2(\gamma + cot2\beta) + 2} \quad (24)$$

Where θ is turning angle, M_1 is Mach number at upward side and β is shock deflection angle

Other flow properties at downward side are calculated by (25-30)given below [3]:

$$M_{n1} = M_1 sin\beta \quad (25)$$

$$M_{n2} = \sqrt{\frac{1+[(\gamma-1)/2]M_{n1}^2}{\gamma M_{n1}^2 - (\gamma-1)/2}} \quad (26)$$

$$M_2 = \frac{M_{n2}}{\sin(\beta-\theta)} \quad (27)$$

$$\frac{P_2}{P_1} = 1 + \frac{2\gamma}{\gamma+1}(M_{n1}^2 - 1) \quad (28)$$

$$\frac{\rho_2}{\rho_1} = \frac{(\gamma+1)M_{n1}^2}{2+(\gamma-1)M_{n1}^2} \quad (29)$$

$$\frac{T_2}{T_1} = \frac{P_2}{P_1}.\frac{\rho_1}{\rho_2} \quad (30)$$

II. LITERATURE REVIEW

By tremendous research during the decade of 1950 to 1960, it was very clear that if we want to eliminate the limitations of rocket and also want to get more performance than a rocket, then the scramjet or air-breathing propulsion is the best choice[1]. In an air-breathing engine for M >1, there are two options available: ramjet engine and scramjet engine but, when operating speed is M >5, then ramjet engine cannot work efficiently due to high losses in intake and very high flow temperature in combustor[1]. Fry [2] showed the efficient operating Mach number range for different propulsion systems with two fuel options: hydrogen and hydrocarbons. Basic oblique and normal shock relations are very useful in inlet design. Anderson [3] states equations of different flow properties based on upstream conditions. Luu Hong Quan et.al.[4] carried out CFD analysis on hypersonic inlets with different No. of ramp against a wide range of Mach number (M=5-10) and analyzed the different flow parameters for all inlets. They proved that an inlet with three ramps is the best choice for a given range of Mach number The performance of the hypersonic inlet also depends on various operating conditions. Augusto F.Moura and Mauricio A.P. Rosa[5] carried out CFD analysis of hypersonic inlet at different operating conditions. Operating conditions that are varied are: operating height, angle of attack, and operating speed. And analyzed the different flow parameters. Except No. of the ramp, ramp angles and other geometrical changes in inlet geometry also impress a huge impact on flow parameters of air passing through inlet. Atulya Sethi [6] carried out CFD analysis on hypersonic inlets with different combinations of No. of ramp and ramp angles at particular Mach number

ISSN No:-2456-2165

And analyzed the different flow parameters. He also compared the values of various flow parameters with values obtained by theoretical equations. Murugesan et.al. [7]] carried out CFD analysis on hypersonic inlets with different geometrical changes like inlets with different No. of the ramp, inlets with same No. of the ramp but varied ramp angles, inlet with different cowl angle and also carried out an analysis on axisymmetric inlets. By analyzing different flow parameters for various inlet geometries, they proved that an inlet with four ramps gives better results than other models for given choices of Mach number Azam che Idris et.al. [8] performed experimental analysis on the hypersonic inlet in a laboratory with different angles of attack and compared the value of various flow parameters with the value obtained by CFD analysis. Murthy, S.N.B, and Curran. E.T [9] have shown performance data of different inlet designs at different Mach number and also discussed major issues related to the hypersonic inlet. Devendra sen et.al.[10] carried out CFD analysis of hypersonic inlet for combined cycle engine for a wide range of Mach number (M=5-8) and found that four ramp inlet is best the choice in terms of pressure recovery and adiabatic efficiency for a given range of Mach number For getting continuous operation at design range of Mach number, inlet must not transfer on unstart state at any Mach number within a range. Qi-Fan Zhang et.al. [11] have shown the process of inlet unstart at low speed, design, and over speed mode.

Research reviews presented above are basically about research works of the hypersonic inlet with $M \geq 5$. So now, when hypersonic inlet has analyzed against very low Mach number, at that time, there are many problems have raised, which we have to face during operation. Kristen Roberts [12] has shown the problems which are raised, when we tasted hypersonic inlet against very low Mach number and also stated some remedies for eliminating those problems and getting good performance. So overall, none of the research was carried out up to now, which analyzed the behavior of hypersonic inlet against very low Mach number and study about different flow parameters and performance parameters for various inlet geometries. This study involves the CFD analysis and technical understanding of various geometries of hypersonic inlets tested against lower starting Mach number (M=3.5). The main objective of this study is to analyze, whether predefined geometries will start against lower speed Mach number (M=3.5) or not? if not then investigate those geometric model(s) technically and find out the reason behind them. In the following sections, the paper will deal with fuel selection, analysis of flow parameters at different sections of a scramjet engine, performance parameters, and efficiencies for different geometries of the inlet which are already tested successfully against lower starting Mach number and compare it with each other.

III. METHODOLOGY

For performing 2-D CFD analysis, first I choose a total of 11 geometries with different combinations of a number of ramp and ramp angles. Here I took the same isolator length for all the geometries. All the geometries are designed at Mach 6 because, after started at a lower starting Mach number (M=3.5), a vehicle will cruise continuously at hypersonic speed i.e. Mach 6. So if we design an inlet at Mach 3.5, then it cannot work with its maximum efficiency at Mach 6 in which the missile will cruise most of the time. Different geometric models are given below:

- **Model :1**

Number of ramp	2
Ramp angles (Degree)	8,7.5
Ramp lengths (mm)	700,704.6
Cowl angle (Degree)	0
Isolator length (mm)	1200

- **Model :2**

Number of ramp	2
Ramp angles (Degree)	8,8
Ramp lengths (mm)	800,767.13
Cowl angle (Degree)	0
Isolator length (mm)	1200

- **Model:3**

Number of ramp	2
Ramp angles (Degree)	8.5,8
Ramp lengths (mm)	700,651.32
Cowl angle (Degree)	0
Isolator length (mm)	1200

- **Model:4**

Number of ramp	2
Ramp angles (Degree)	9,8
Ramp lengths (mm)	700,633.48
Cowl angle (Degree)	0
Isolator length (mm)	1200

- **Model:5**

Number of ramp	3
Ramp angles (Degree)	7.6,7,6
Ramp lengths (mm)	700,278.75,348.37
Cowl angle (Degree)	0
Isolator length (mm)	1200

ISSN No:-2456-2165

- **Model:6**

Number of ramp	3
Ramp angles (Degree)	8.15,7,6
Ramp lengths (mm)	700,267.56,373.34
Cowl angle (Degree)	0
Isolator length (mm)	1200

- **Model:7**

Number of ramp	3
Ramp angles (Degree)	8.3,7.3,6
Ramp lengths (mm)	700,278.57,381.1
Cowl angle (Degree)	0
Isolator length (mm)	1200

- **Model:8**

Number of ramp	3
Ramp angles (Degree)	8.5,7,6
Ramp lengths (mm)	700,267.07,303.68
Cowl angle (Degree)	0
Isolator length (mm)	1200

- **Model:9**

Number of ramp	4
Ramp angles (Degree)	7,6,5,4
Ramp lengths (mm)	800,331.17,157.7,345.78
Cowl angle (Degree)	0
Isolator length (mm)	1200

- **Model:10**

Number of ramp	4
Ramp angles (Degree)	7,6.5,5,4.5
Ramp lengths (mm)	800,323.11,152.76,315.86
Cowl angle (Degree)	0
Isolator length (mm)	1200

- **Model:11**

Number of ramp	4
Ramp angles (Degree)	8,7,6.5,5
Ramp lengths (mm)	800,318.5,142.13,243.6
Cowl angle (Degree)	0
Isolator length (mm)	1200

3.2 Free stream condition

Here it is assumed that hypersonic vehicle is cruise in constant dynamic pressure trajectory, which has dynamic pressure of 47880 N/m^2. This value is directly taken from reference [12]. By taken dynamic pressure and Mach number as input values, we can calculate corresponding pressure and temperature at particular height. Flow properties at each Mach number on constant dynamic pressure trajectory are given below:

Table 3: Pressure and temperature of air at different Mach number for same dynamic pressure

Mach number	Height (m)	$T_0\ (K)$	$P_0\ (Pa)$
3.5	19936.97	216.65	5582
4	21646.90	218.22	4275
4.5	23167.85	219.73	3377
5	24539.45	221.09	2736
5.5	25786.08	222.33	2260
6	26929.08	223.47	1900

There are many other parameters used in stream thrust analysis, some of them has constant value throughout the analysis and some of them has assumed value. List of these values are given below and directly taken from reference [12]:

Table 4: List of constant parameters used in stream thrust analysis

Constants [12]	
C_{pc}	$1090\ J/kgK$
R	$289.3\left(\frac{m}{s}\right)^2/K$
C_{pb}	$1510\ J/kgK$
C_{pe}	$1510\ J/kgK$
h_f	0.00
g_0	$9.81\ m/s^2$

Table 5: List of assumed parameters used in stream thrust analysis

Assumed values [12]			
V_{fx}/V_3	0.50	T^0	222.0 K
V_f/V_3	0.50	P_{10}/P_0	1.40
$C_f * A_w/A_3$	0.10	γ_c	1.362
η_c	0.90	γ_b	1.238
η_b	0.90	γ_e	1.238
η_e	0.90		

3.2 Computational Domain

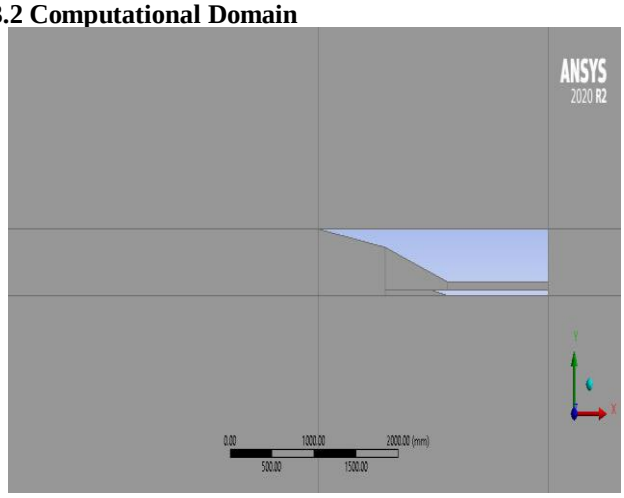

Fig. 3.2.1: Computational fluid domain for 2 ramp inlet geometry

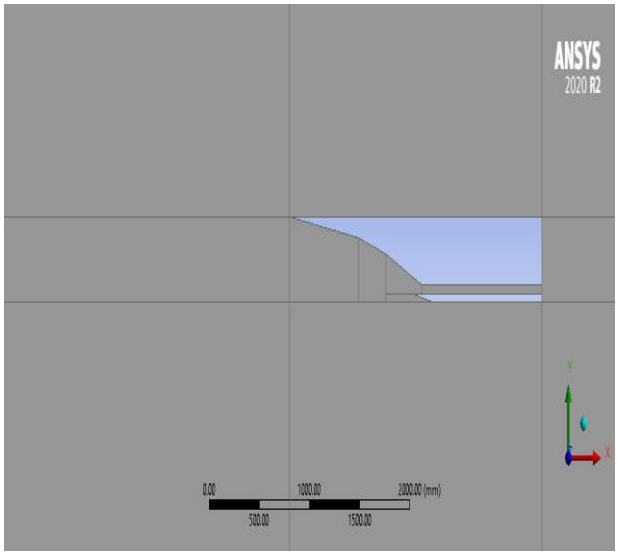

Fig. 3.2.2: Computational fluid domain for 3 ramp inlet geometry

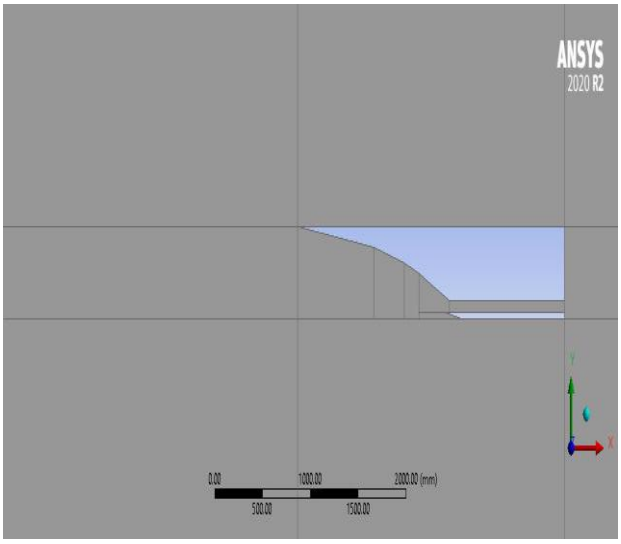

Fig. 3.2.3: Computational fluid domain for 4 ramp inlet geometry

Here as shown in figures given above, inlet geometry is bounded by the main rectangular fluid domain which is further divided into sub-domains. Here I generated a separate sub-domain for all the ramps and also for the isolator, for catching shocks and their interaction and also for getting better accuracy of results. I also generated sub-domain at an upper and lower portion of inlet geometry for catching flow spillage happened at off-design conditions.

3.3 Meshing

For carried out 2-D simulation over inlet geometry, a structured grid with quadrilateral cells is made. All the sub-domains of geometry consist of a structured grid. There are more than 32000 nodes in each geometric model of the inlet. Sub-domains of ramp and isolator consist of fine mesh for capturing shocks in a better way, while upper and lower sub-domain of inlet geometry consists of medium mesh.

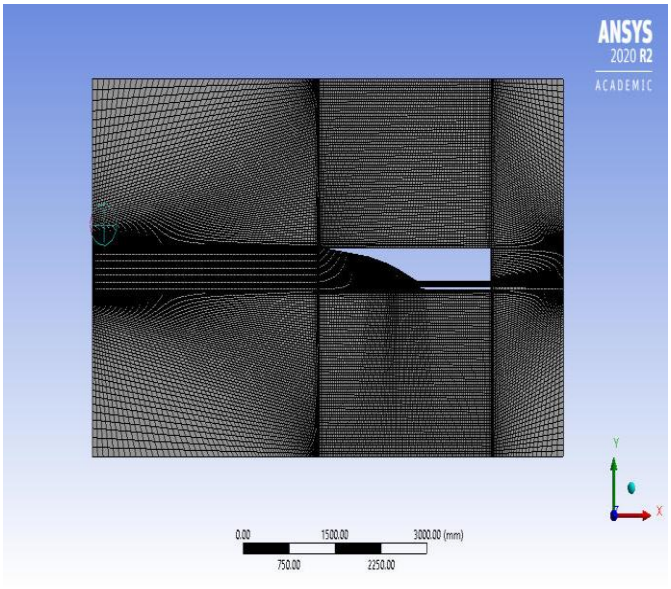

(a)

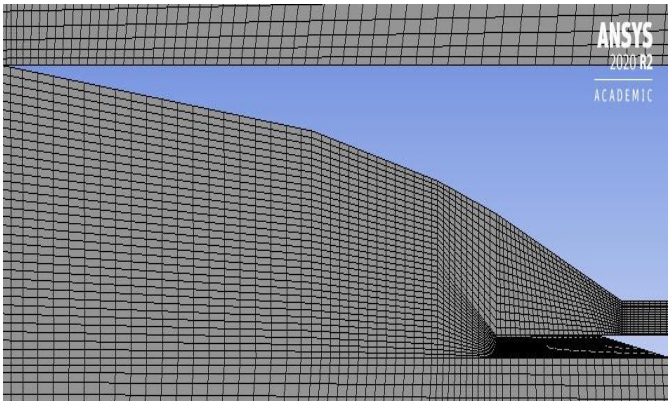

(b)

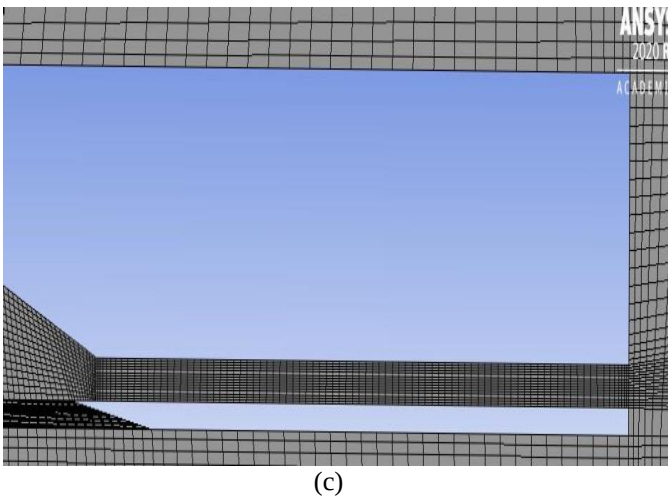

(c)

Fig. 3.3.1: Mesh at different sections of 4 ramp inlet design.

IV. RESULTS AND DISCUSSION

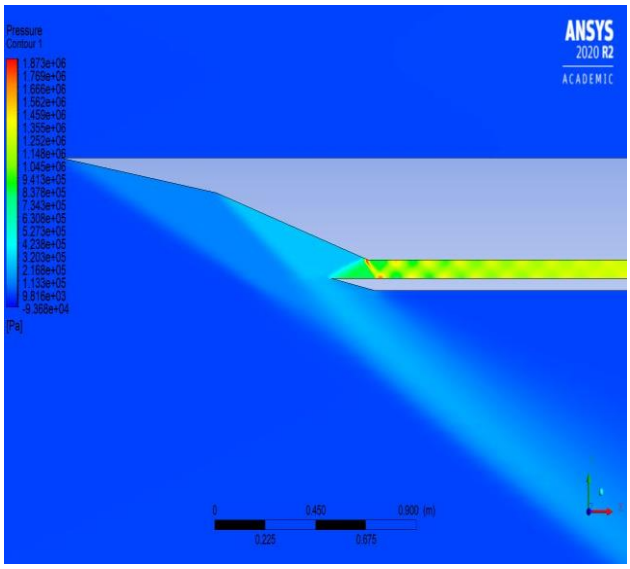

Fig. 4.1:Pressure contour of model 1 at Mach3.5

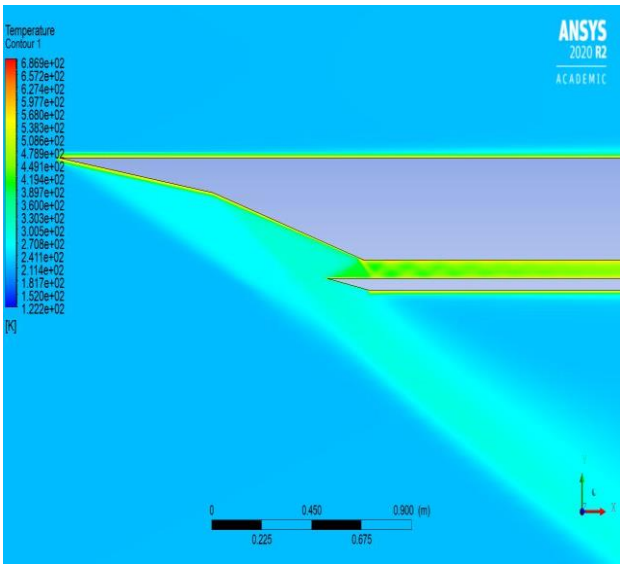

Fig. 4.2:Temperature contour of model 1 at Mach 3.5

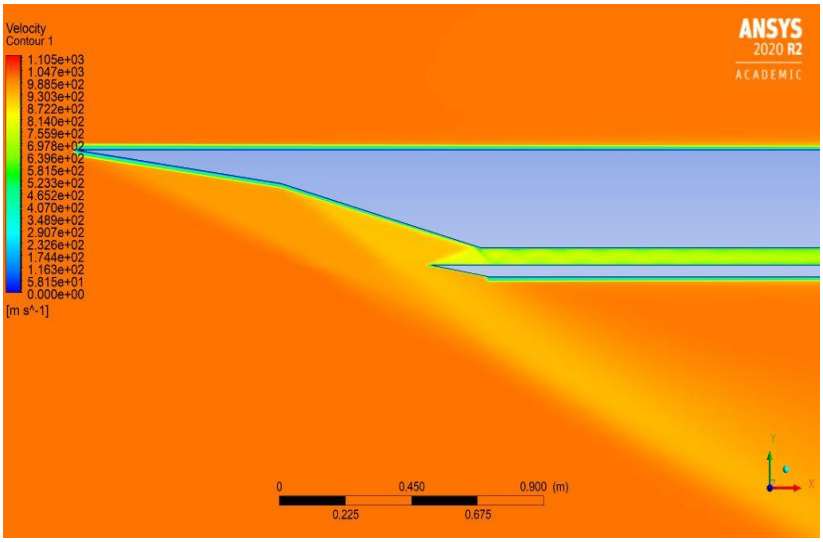

Fig. 4.3:Velocity contour of model 1 at Mach 3.5

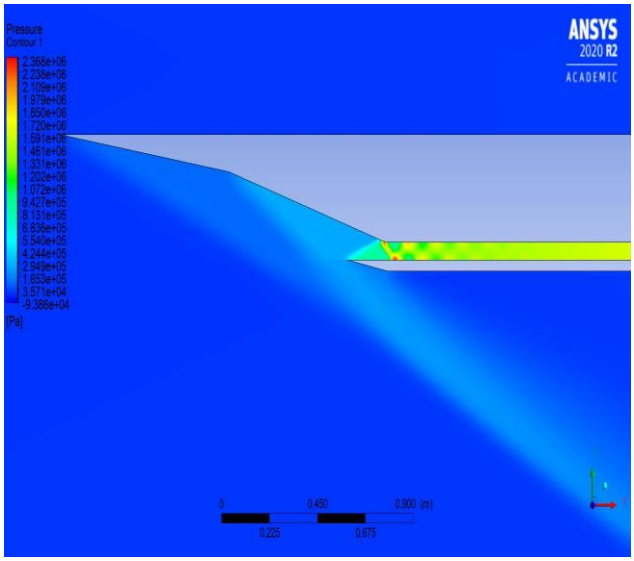

Fig. 4.4:Pressure contour of model 2 at Mach3.5

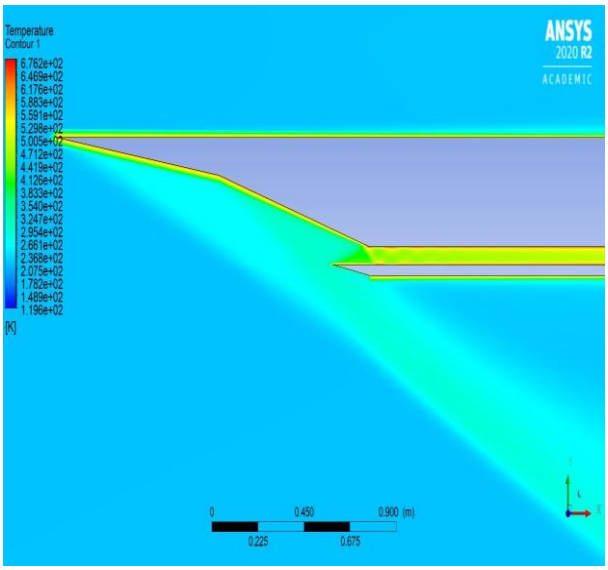

Fig. 4.5:Temperature contour of model 2 at Mach 3.5

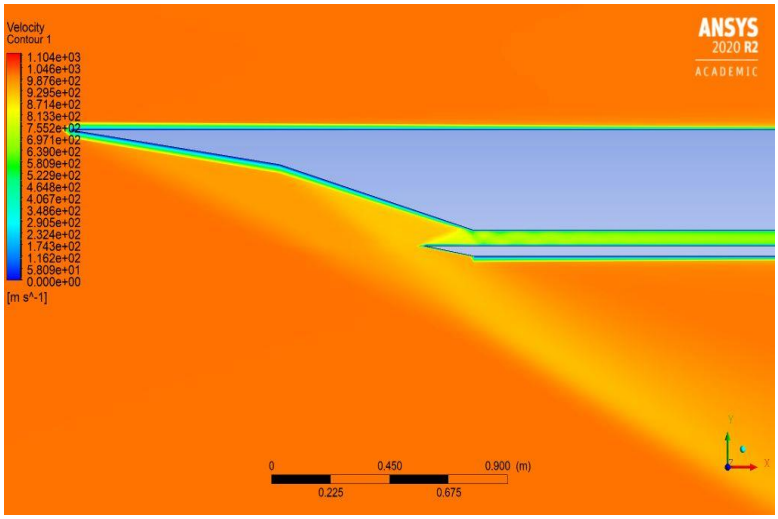

Fig. 4.6:Velocity contour of model 2 at Mach 3.5

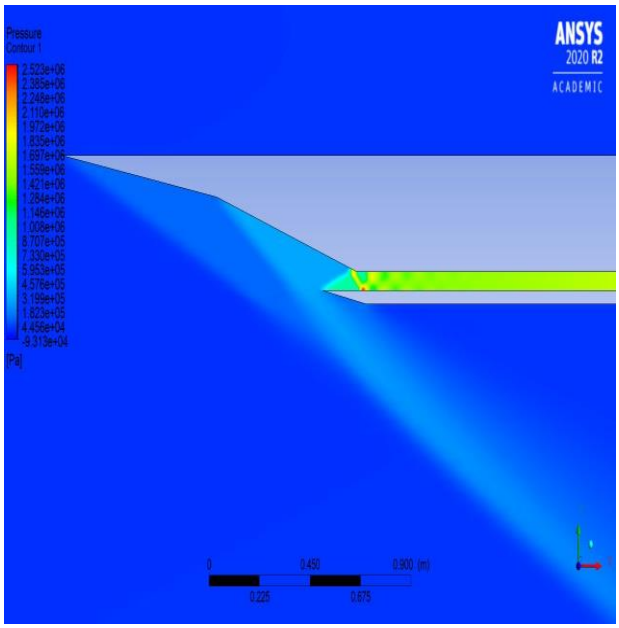

Fig. 4.7:Pressure contour of model 3 at Mach3.5

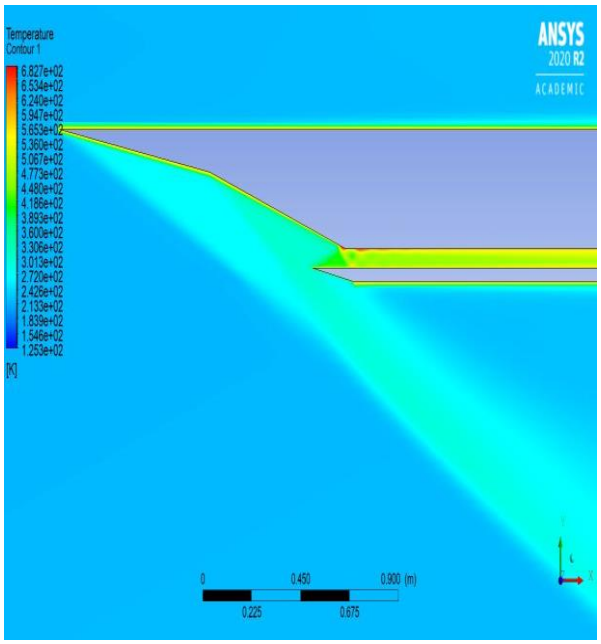

Fig. 4.8:Temperature contour of model 3 at Mach 3.5

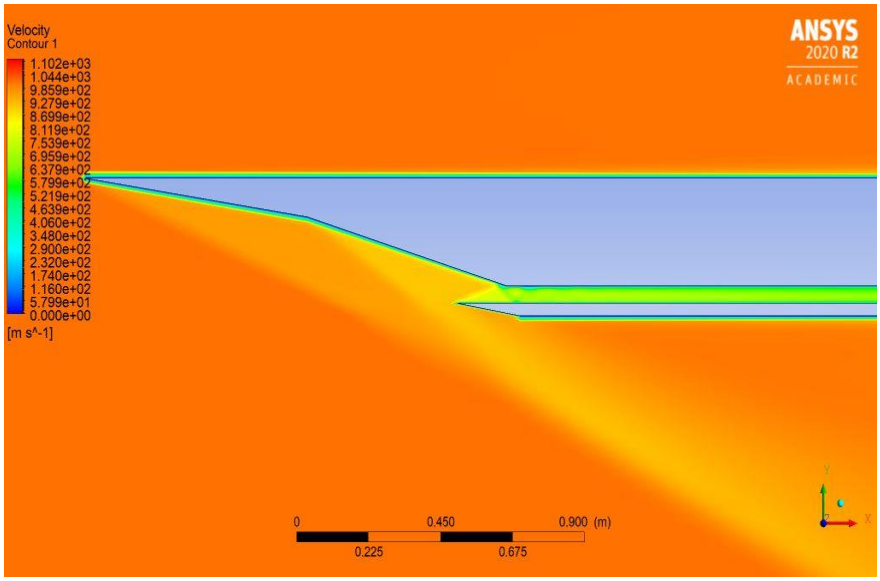

Fig. 4.9:Velocity contour of model 3 at Mach 3.5

ISSN No:-2456-2165

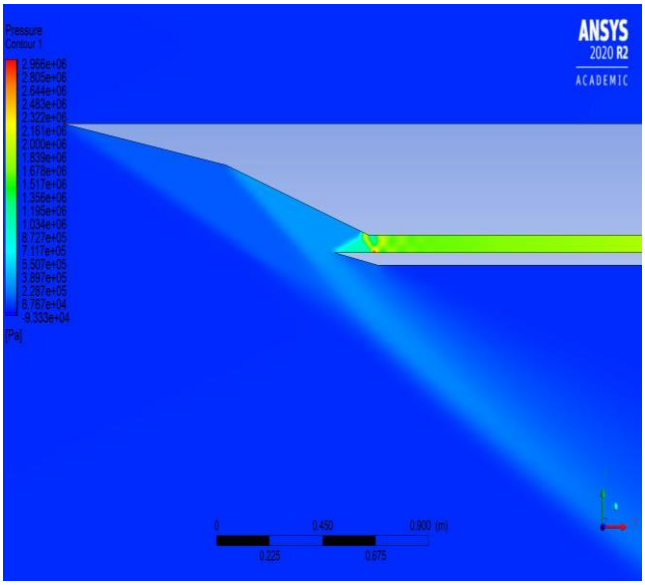

Fig. 4.10:Pressure contour of model 4 at Mach3.5

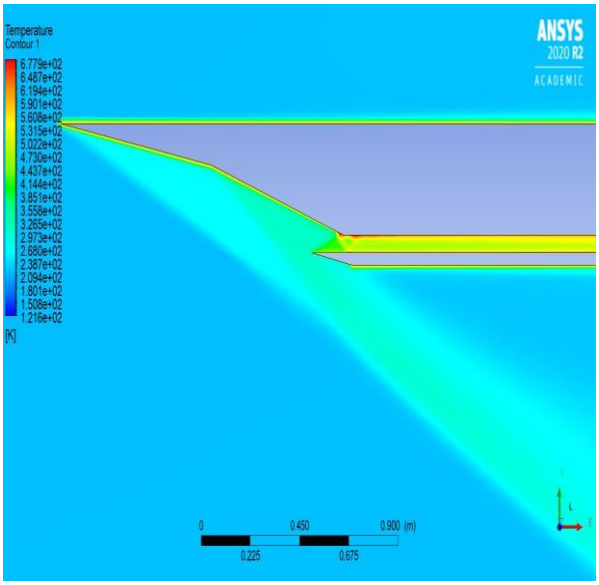

Fig. 4.11:Temperature contour of model 4 at Mach3.5

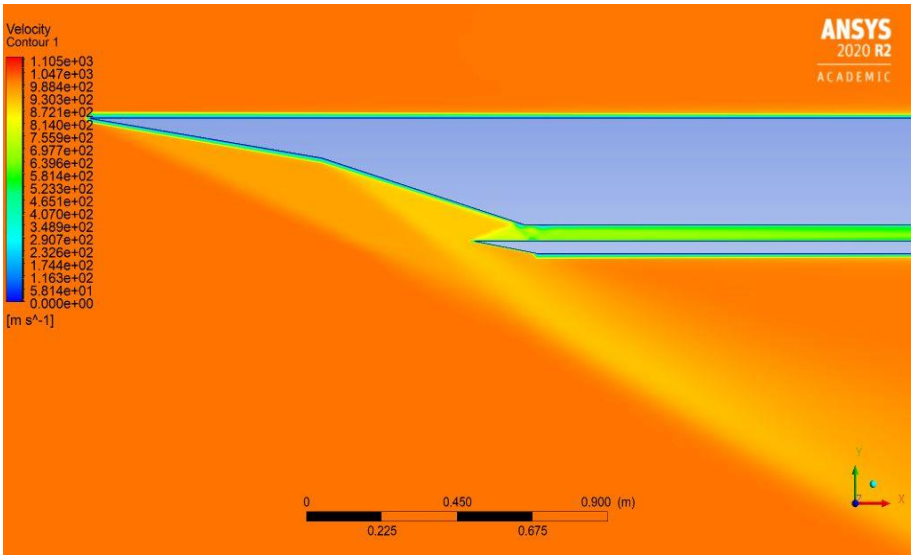

Fig. 4.12:Velocity contour of model 4 at Mach 3.5

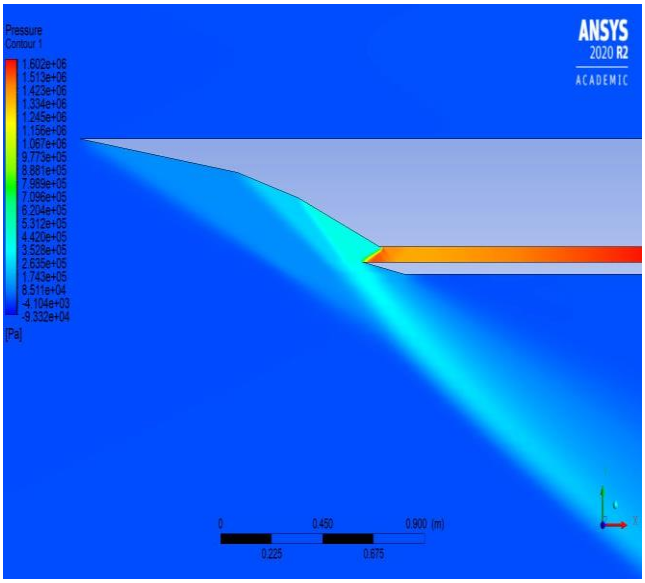

Fig. 4.13:Pressure contour of model 5 at Mach3.5

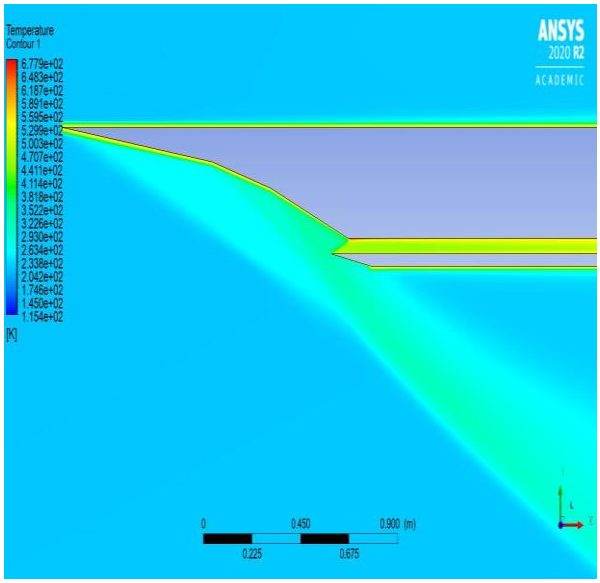

Fig. 4.14:Temperature contour of model 5 at Mach3.

ISSN No:-2456-2165

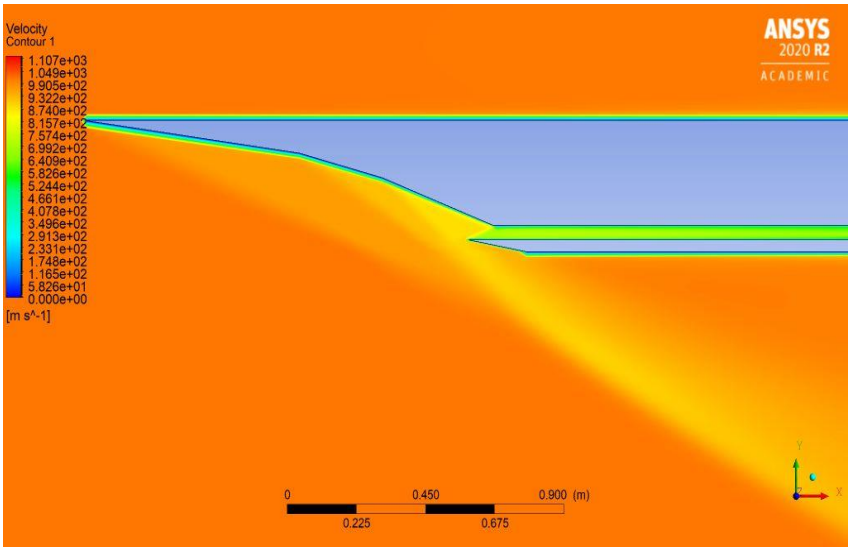

Fig. 4.15:Velocity contour of model 5 at Mach 3.5

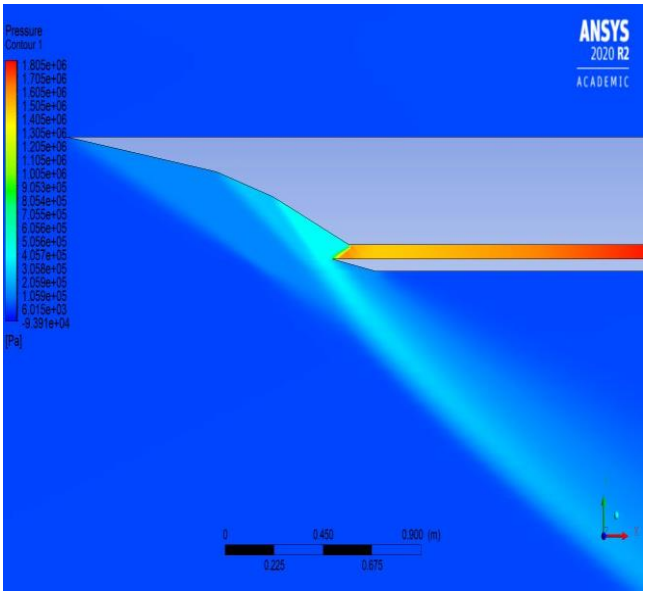

Fig. 4.16:Pressure contour of model 6 at Mach3.5

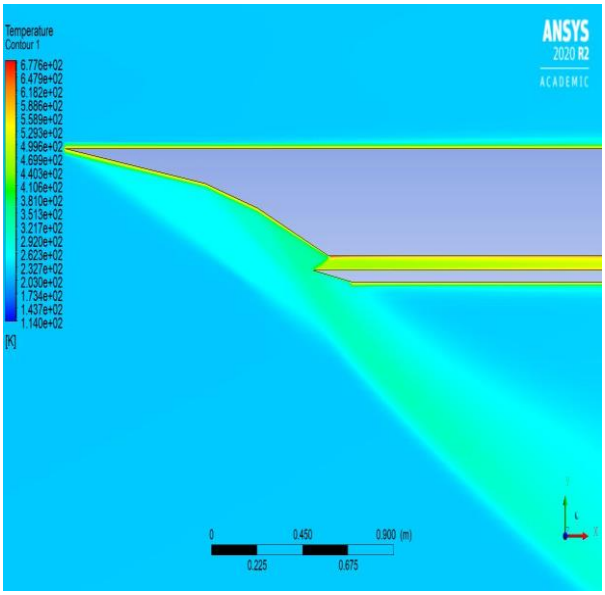

Fig. 4.17:Temperature contour of model 6 at Mach3.5

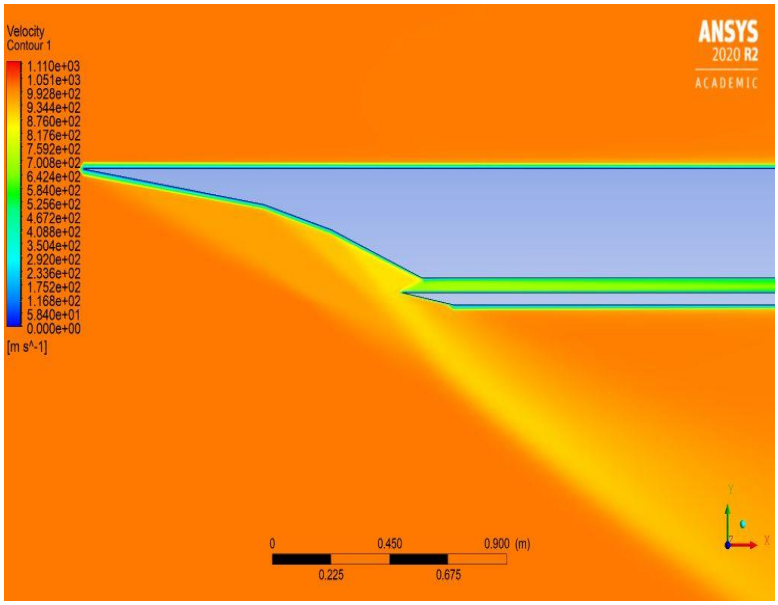

Fig. 4.18:Velocity contour of model 6 at Mach 3.5

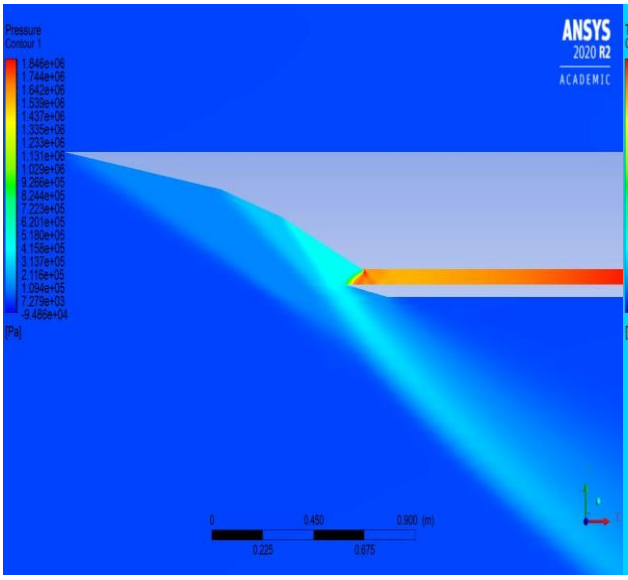

Fig. 4.19:Pressure contour of model 7 at Mach3.5

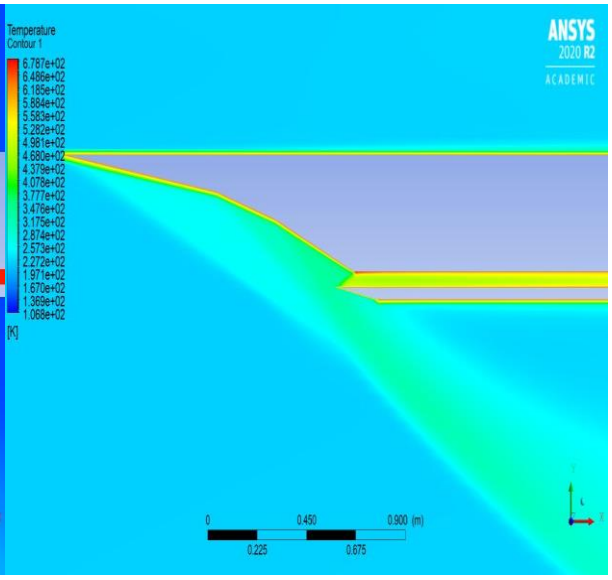

Fig. 4.20:Temperature contour of model 7 at Mach 3.5

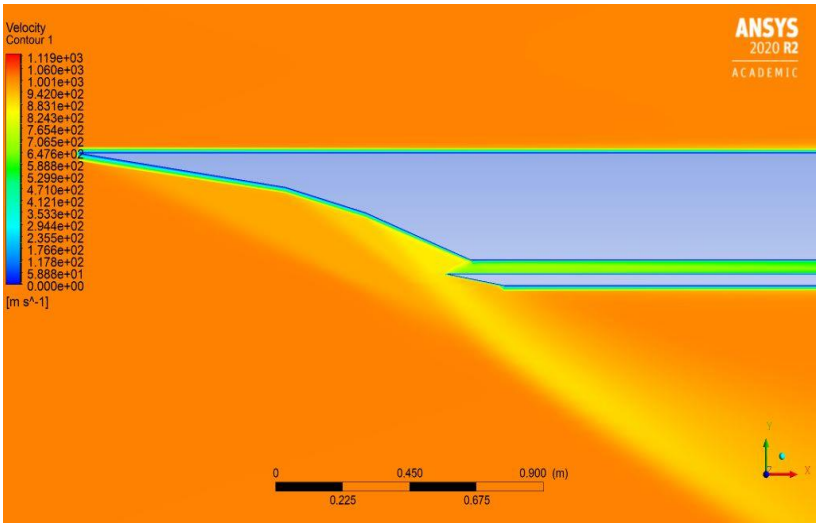

Fig. 4.21:Velocity contour of model 7 at Mach 3.5

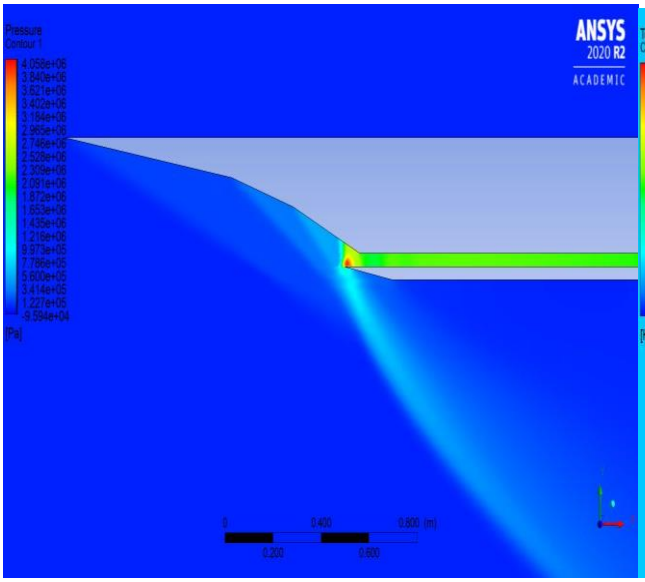

Fig. 4.22:Pressure contour of model 8 at Mach3.5

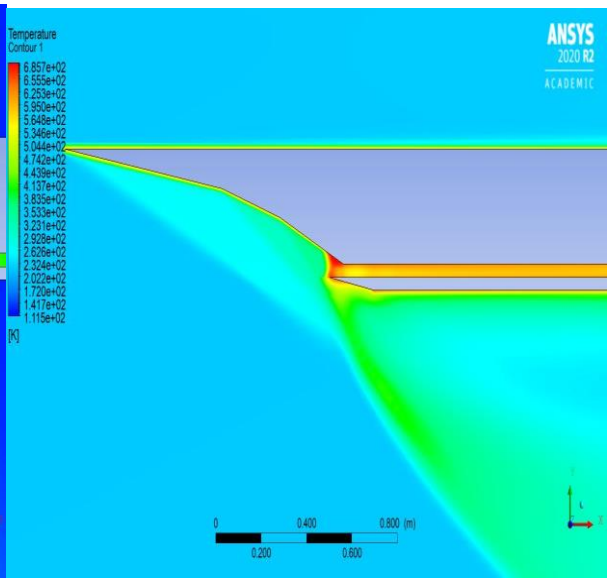

Fig. 4.23:Temperature contour of model 8 at Mach 3.5

ISSN No:-2456-2165

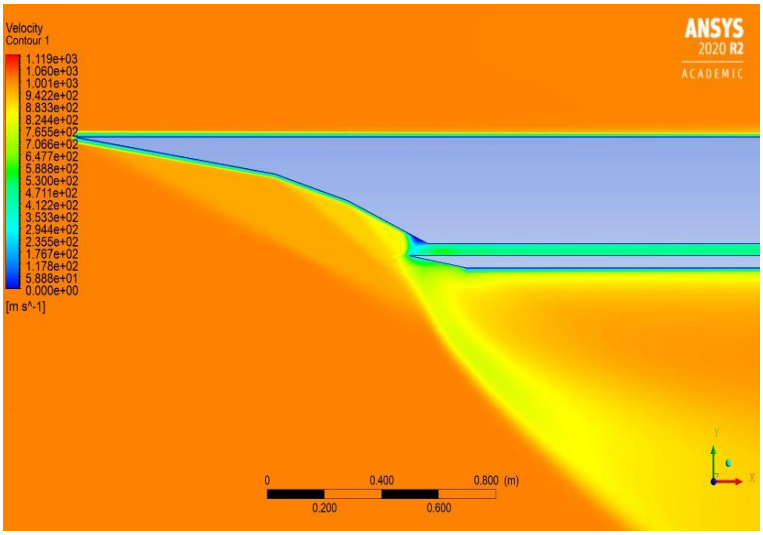

Fig. 4.24:Velocity contour of model 8 at Mach 3.5

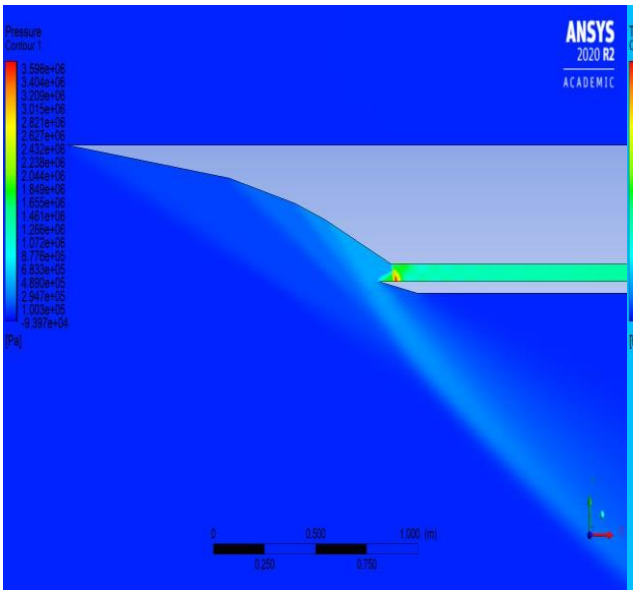

Fig. 4.25:Pressure contour of model 8 at Mach3.5

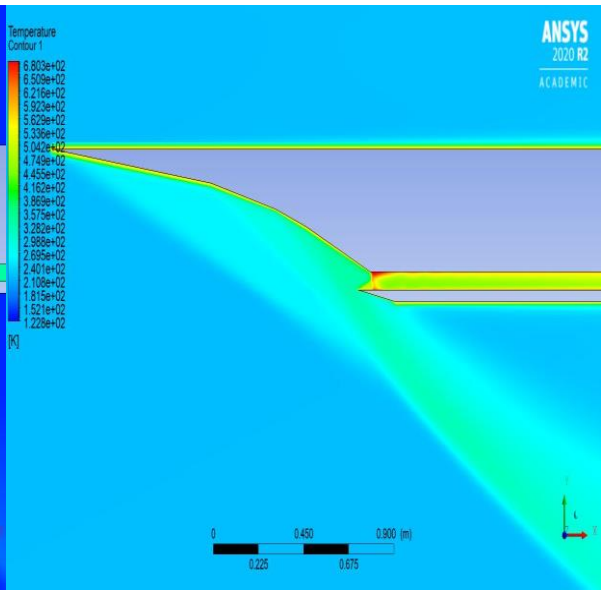

Fig. 4.26:Temperature contour of model 9 at Mach 3.5

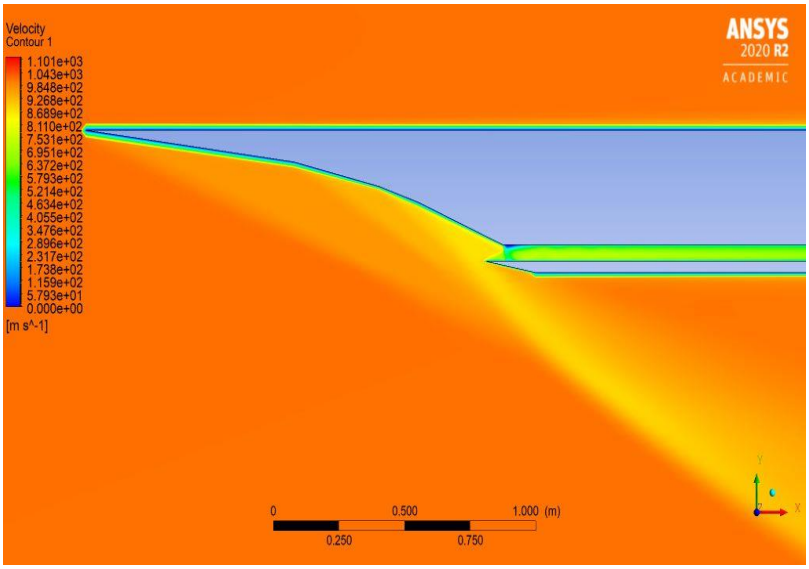

Fig. 4.27:Velocity contour of model 9 at Mach 3.5

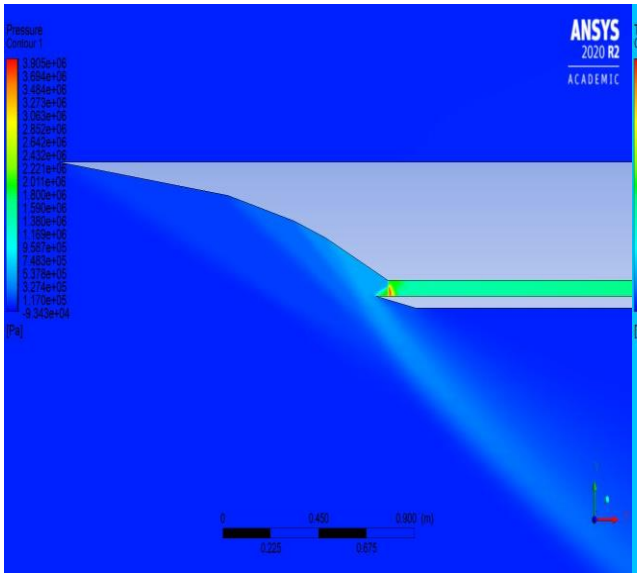

Fig. 4.28:Pressure contour of model 10 at Mach3.5

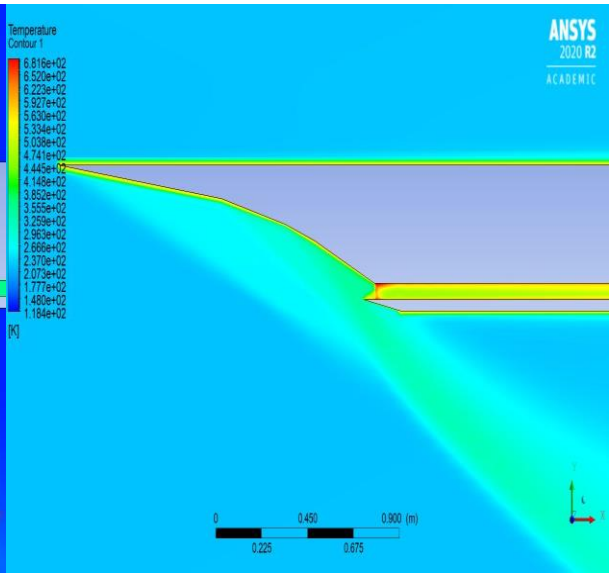

Fig. 4.29:Temperature contour of model 10 at Mach 3.5

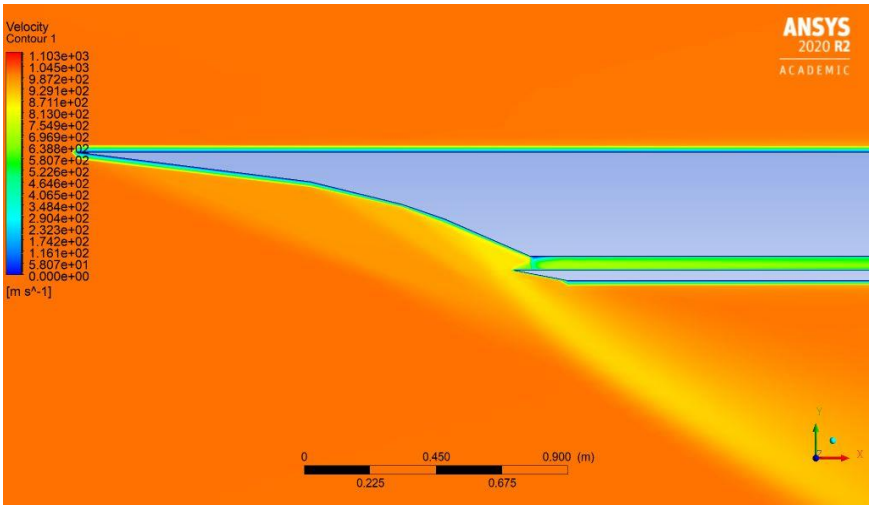

Fig. 4.30:Velocity contour of model 10 at Mach 3.5

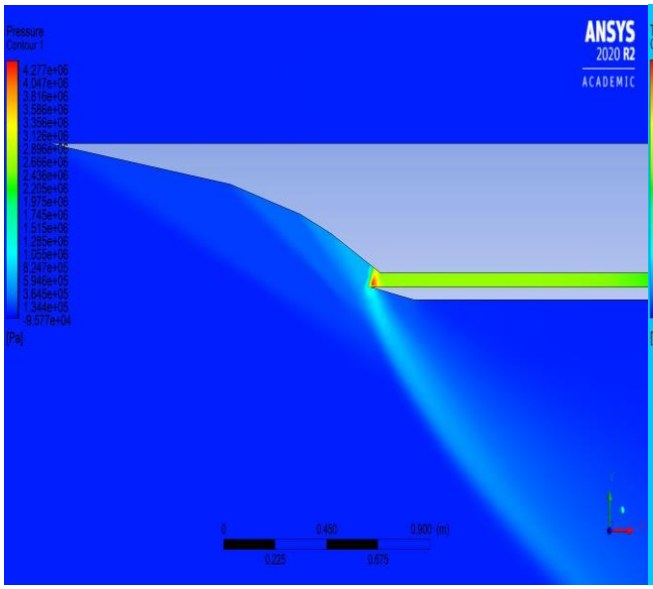

Fig. 4.31:Pressure contour of model 11 at Mach3.5

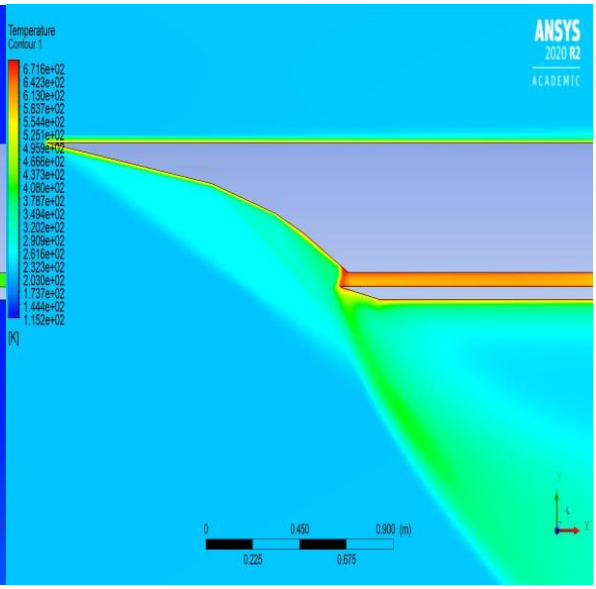

Fig. 4.32:Temperature contour of model 11 at Mach 3.5

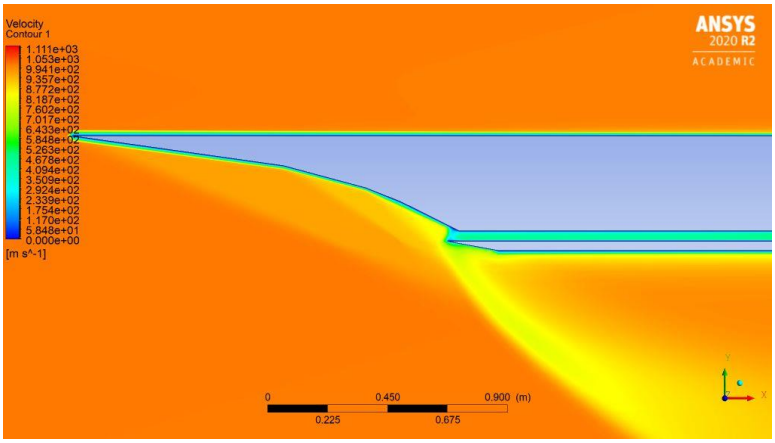

Fig. 4.33:Velocity contour of model 11 at Mach 3.5

Here in all two ramps design i.e. model 1,2,3&4, flow spillage is clearly seen, as these simulations are carried out at Mach 3.5 i.e. below the design Mach number. All the shocks are attached throughout the whole inlet body. Here we can clearly see that shocks are reflected inside the isolator only up to some part of the total length, so it will not affect the combustion process happening inside the combustor. Flow separation has not happened inside the isolator because there is no shocks interaction formed inside it. As per the cases of two ramp designs, flow spillage also happened in the cases of three ramp designs. In the case of model 5,6&7, all the shocks are attached throughout the whole inlet body but in model 8, shock is detached near the end part of the third ramp. This shock detachment happened because of the comparatively larger deflection angle of ramps. Here no shock penetration happened inside the isolator, so the combustor will get flow with uniform flow properties. There is no flow separation happened in the case of model 5,6&7 but due to shock detachment, significant flow separation is visible in the case of model 8. As same as previous cases, we can clearly see the flow spillage also in four ramp designs. . In the case of models 9&10, shocks are attached throughout the inlet body but in the case of model 11, shock detachment has happened. Shock penetration inside the isolator has not happened also in four ramp designs. Minor flow separation is visible in the case of models 9&10 because of somewhat larger ramp angles according to intake airflow velocity.

In all three types of design i.e. 2 ramps, 3 ramps &4 ramps intake designs, as ramp angles are increase, temperature and pressure are going to increase while velocity is going to decrease because as the ramp angles go higher, oblique shocks will become more stronger. The cases in which shock detachment happened, a large velocity drop at a place of detachment is shown in those corresponding cases. So pressure recovery is also very low in those cases. Isolator helped to increase pressure and temperature up to the required value. The role of the isolator here in this type of crucial case, where some required values of pressure and temperature must be needed is so important.

Values of different flow parameters at various stations and performance parameters of scramjet engine at Mach 3.5 for all models are given below:

Table 6: List of different flow and performance parameters obtained at the end of stream thrust analysis for Mach 3.5

Model No.	**No. of Ramp**	**Ramp Angles**	T_3 **(K)**	V_3 $(\frac{m}{sec})$	P_3 **(Mpa)**	T_4 **(K)**	V_4 $(\frac{m}{sec})$	M_4
1	2	(8,7.5)	460	725	1.35	-	-	-
2	2	(8,8)	490	660	1.65	1185	652.84	1.0004
3	2	(8.5,8)	490	655	1.70	1160.4	649.94	1.0018
4	2	(9,8)	512	625	1.86	1033.2	611.875	1.0041
4	2	(9,8)	512	625	1.86	1036.9	611.875	1.0024
5	3	(7.6,7,6)	487	662	1.61	1192	655.20	1.0011
6	3	(8.15,7,6)	510	635	1.80	1081.1	623.50	1.0003
6	3	(8.15,7,6)	510	635	1.80	1060.1	622.585	1.0087
7	3	(8.3,7.3,6)	512	630	1.85	1058.1	617.683	1.0017
7	3	(8.3,7.3,6)	512	630	1.85	1057	617.5	1.0019
8	3	(8.5,7,6)	575	535	1.875	1094	523.765	0.8353
8	3	(8.5,7,6)	575	535	1.875	1097.7	523.765	0.8339
9	4	(7,6,5,4)	487	663	1.40	1196.8	656.383	1.0009
10	4	(7,6.5,5,4.5)	513	620	1.63	1034.2	611.875	1.0037
10	4	(7,6.5,5,4.5)	513	620	1.63	1037.8	611.875	1.0019
11	4	(8,7,6.5,5)	575	530	2.1	1094	518.87	0.8275
11	4	(8,7,6.5,5)	575	530	2.1	1097.7	518.87	0.8216

T_{10} (K)	V_{10} $(\frac{m}{sec})$	$F/\dot{m}$ $(N\,s\,/kg)$	Sp.fuel consumption $(\frac{kg}{N\,s})$	Fuel	Fuel to Air Ratio (f)	η_0	η_{th}	η_P	Isp (sec)	Possible or Not
-	-	-	-	Octane	-	-	-	-	-	Not
500	1579.8	633.23	4.264×10^{-5}	Octane	0.027	0.5325	0.6322	0.8423	2390.6	Yes
487.225	1565.8	616.78	4.215×10^{-5}	Octane	0.026	0.5386	0.6360	0.847	2418	Yes
428.14	1483.3	521.65	3.834×10^{-5}	Octane	0.02	0.5922	0.6763	0.8757	2658.6	Yes
426.66	1486	523.93	3.817×10^{-5}	Hexane	0.02	0.5907	0.6753	0.8748	2670.5	Yes
504.44	1582.8	637.21	4.3×10^{-5}	Octane	0.0274	0.5281	0.6274	0.8416	2370.8	Yes
450.12	1514.7	556.958	3.95×10^{-5}	Octane	0.022	0.5748	0.6650	0.8644	2580.5	Yes
441.384	1502	542.22	3.873×10^{-5}	Hexane	0.021	0.5822	0.6701	0.8688	2632	Yes
438.81	1500.6	540.676	3.884×10^{-5}	Octane	0.021	0.5846	0.6725	0.8693	2624.5	Yes
438.337	1500	539.582	3.854×10^{-5}	Hexane	0.0208	0.585	0.6728	0.8694	2644.7	Yes
-	-	-	-	Octane	0.02	-	-	-	-	Not
-	-	-	-	Hexane	0.02	-	-	-	-	Not
517.051	1576	631.3	4.372×10^{-5}	Octane	0.0276	0.5194	0.6141	0.8458	2331.8	Yes
436.9	1476	514.206	3.89×10^{-5}	Octane	0.02	0.5838	0.663	0.8806	2620.9	Yes
438.45	1478	516.47	3.872×10^{-5}	Hexane	0.02	0.5823	0.6619	0.8797	2632.5	Yes
-	-	-	-	Octane	0.02	-	-	-	-	Not
-	-	-	-	Hexane	0.02	-	-	-		Not

Here I used octane and hexane as fuel according to the airflow temperature I got at the exit of the isolator. So according to the allowable equivalence ratio as mentioned in the previous section, the allowable range for variation of fuel-to-air ratio is 0.02-0.0664 for octane and 0.02-0.0659 for hexane

In model 1, airflow temperature at the exit of isolator did not reach up to the ignition temperature of fuels, so model 1can not work in the condition of lower starting Mach number. In models 8 & 11, even at the lowest possible fuel-to-air ratio, the Mach number at the combustor exit did not reach above Mach 1. So model 8 & 11 also cannot work in the condition of lower starting Mach number, as must be greater than 1 in case of the scramjet engine. Here I took the best cases from all three types of intake design i.e. 1-ramp, 2-ramp & 3-ramp design for further analysis on the basis of the value of $F/\dot{m}$. So that models 2,5 & 9 are selected for further analysis at Mach 6.

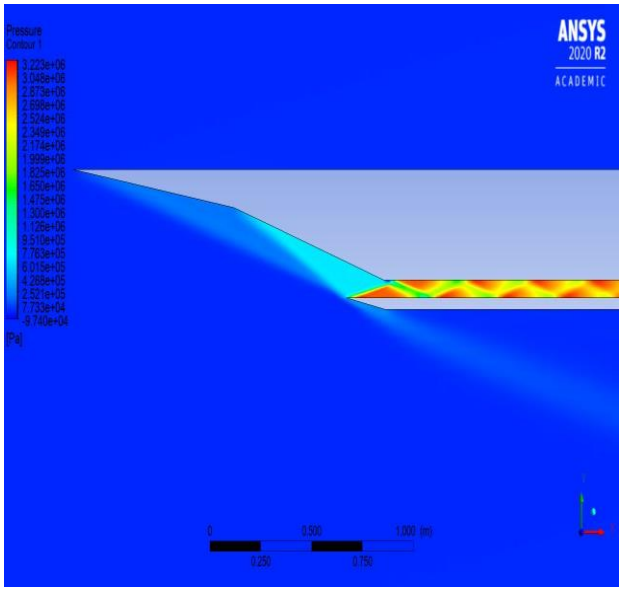

Fig. 4.45:Pressure contour of model 2 at Mach 6

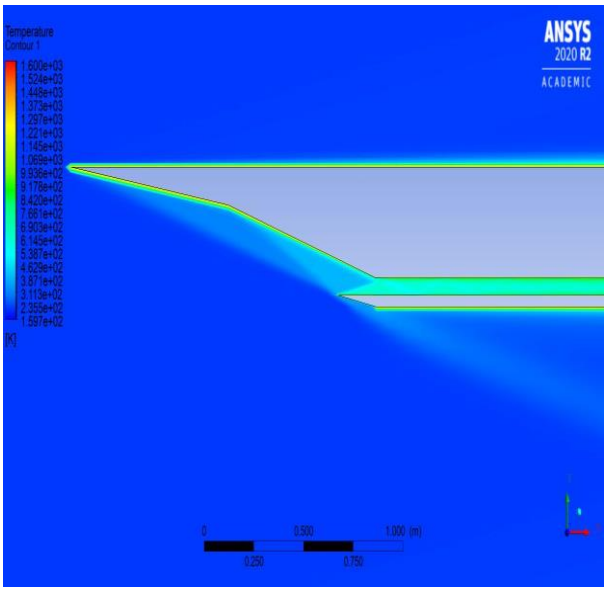

Fig. 4.46:Temperature contour of model 2 at Mach 6

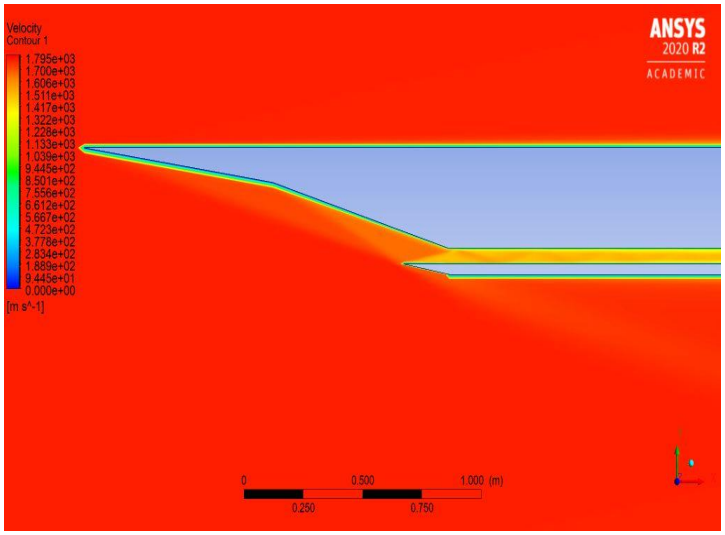

Fig. 4.47:Velocity contour of model 2 at Mach 6

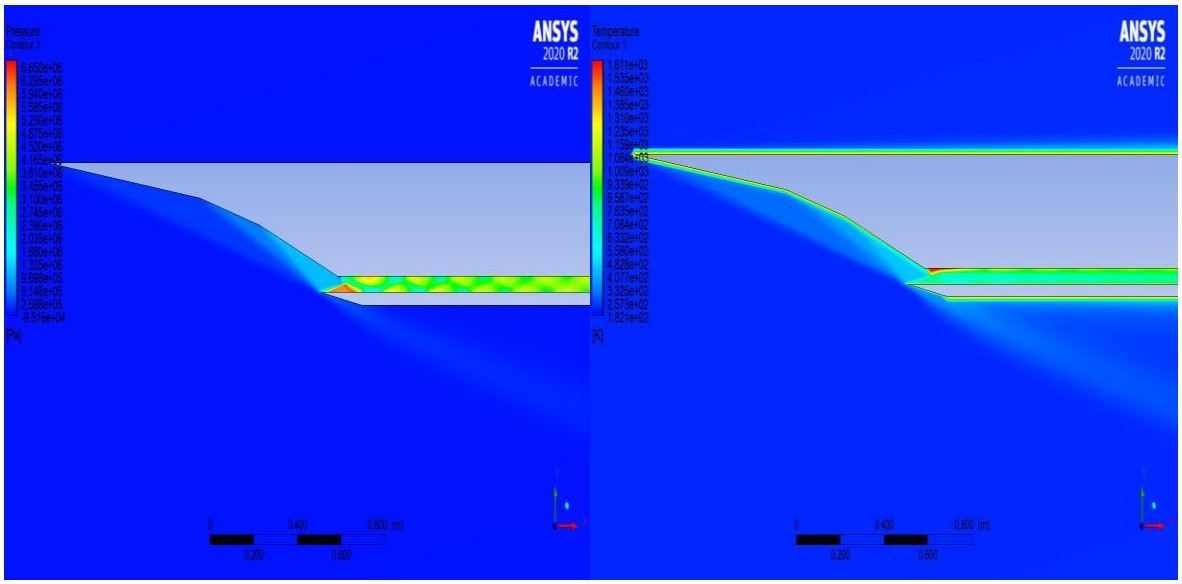

Fig. 4.48:Pressure contour of model 5 at Mach 6

Fig. 4.49:Temperature contour of model 5 at Mach 6

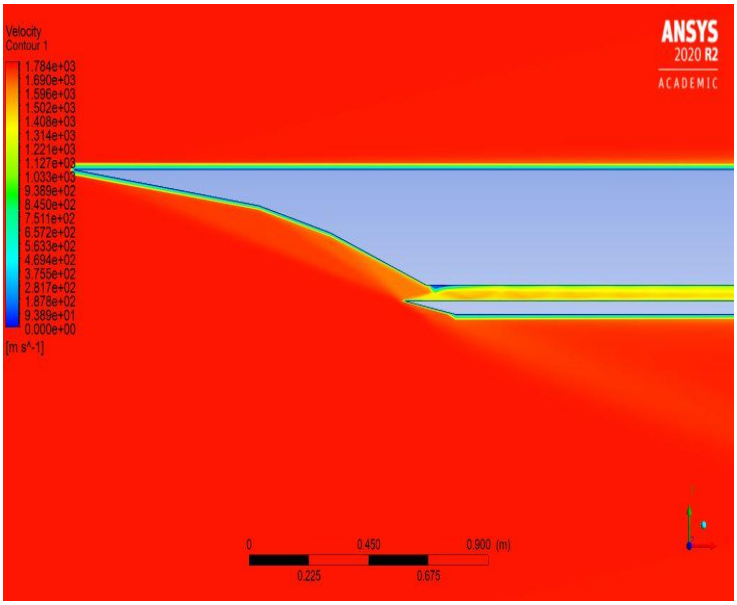

Fig. 4.50:Velocity contour of model 5 at Mach 6

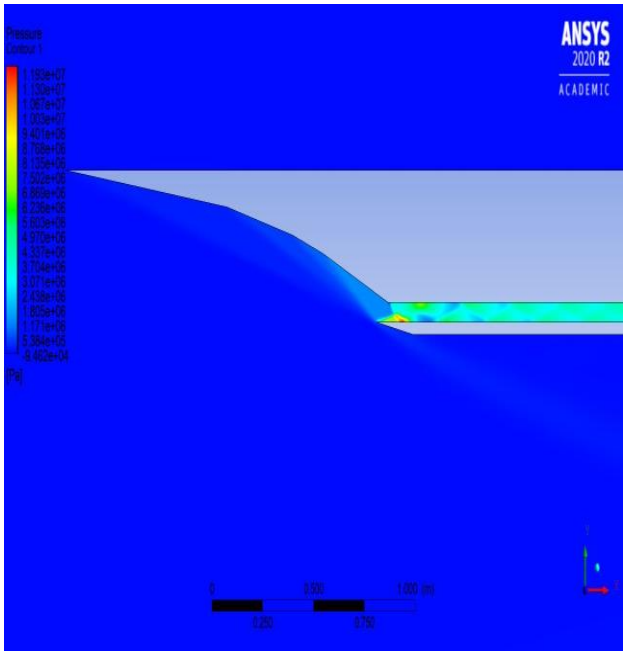

Fig. 4.51:Pressure contour of model 9 at Mach 6

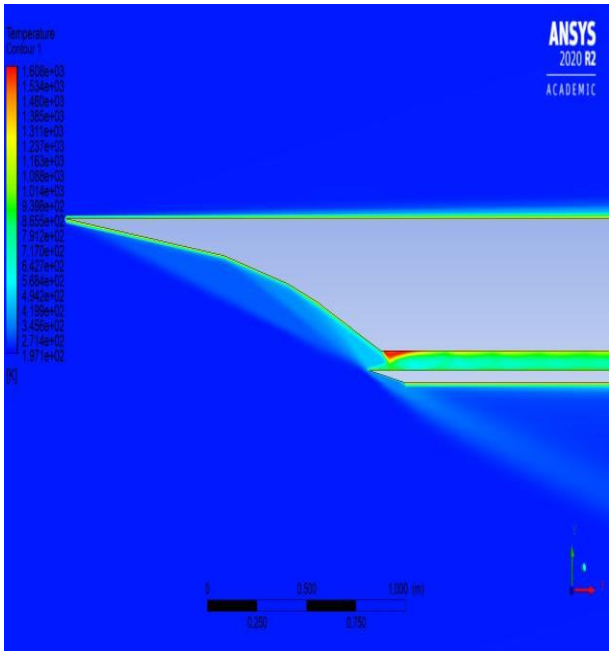

Fig. 4.52:Temperature contour of model 9 at Mach 6

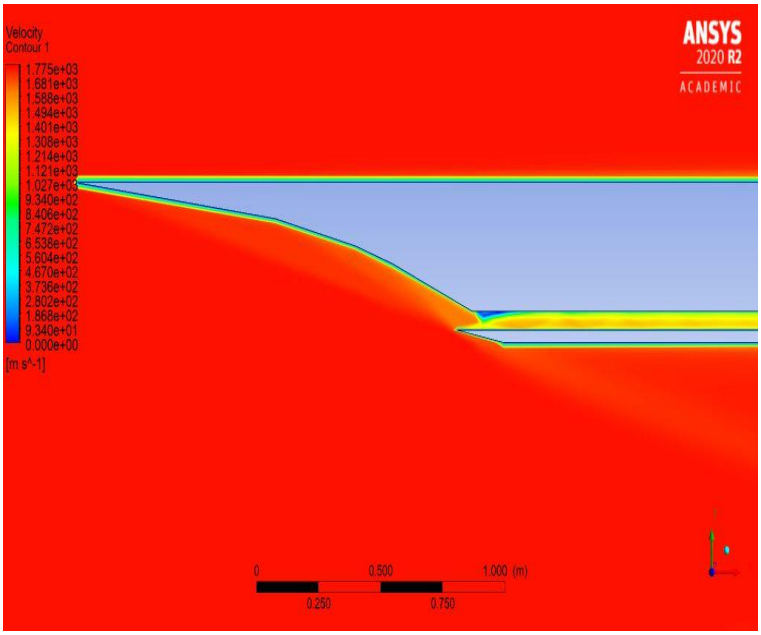

Fig. 4.53:Velocity contour of model 9 at Mach 6

Here all three designs i.e. model no 2,5 & 9 operating at design Mach number (M= 6), so that all the shocks have impinged exactly at the cowl tip. Due to shock on lip condition exist, there is no flow spillage has happened in these cases. The boundary layer at the vehicle forebody and ramp walls are thinner than the boundary layer at Mach 3.5. It is clearly visible that the shock train is propagating inside the isolator so that pressure and temperature are increased and velocity is decreased at the end of the isolator due to flow passes through the continuous shock train. There is minor flow separation at the upper wall of the isolator is visible in case of model numbers 5&9

As shown in the figures, temperature and pressure at end of the isolator are quite higher in 3 & 4 ramp designs than in 2-ramp design, while velocity is higher in 2-ramp design because of the higher pressure ratio of 3 & 4 ramp inlet designs. Whereas the performance of 3 & 4 ramp inlet designs in terms of flow parameters is quite similar to each other. Shock train propagation inside the isolator is clearly visible in the graphs. Values of different flow parameters at various stations and performance parameters of scramjet engine at Mach 3.5 for all models are given below:

ISSN No:-2456-2165

Table 7: List of different flow and performance parameters obtained at the end of stream thrust analysis for Mach 6

Model No.	No. of Ramp	Ramp Angles	T_3 (K)	V_3 $(\frac{m}{sec})$	P_3 (Mpa)	T_4 (K)	V_4 $(\frac{m}{sec})$	M_4
2	2	(8,8)	632	1490	2.70	2164.6	1559	1.7675
5	3	(7.6,7,6)	780	1380	4	2318.2	1443.9	1.582
9	4	(7,6,5,4)	800	1380	3.75	2337	1444	1.5755

T_{10} (K)	V_{10} $(\frac{m}{sec})$	$F/\dot{m}$ (Ns/kg)	Sp.fuel consumption $(\frac{kg}{Ns})$	Fuel	Fuel to Air Ratio (f)	η_0	η_{th}	η_P	Isp (sec)	Possible or Not
731.42	2600	1027.4	6.462×10^{-5}	Octane	0.0664	0.6117	0.6848	0.8933	1577.3	Yes
743.2	2615.6	1044.6	6.356×10^{-5}	Octane	0.0664	0.6219	0.6996	0.8890	1603.6	Yes
755.637	2619.2	1048.8	6.33×10^{-5}	Octane	0.0664	0.6245	0.7030	0.8883	1610.3	Yes

Herein all the cases, I used stoichiometric fuel-to-air ratio for measuring performance parameters. Graphs of performance parameters of these selected models for the whole Mach number range i.e. 3.5 to 6 are given below:

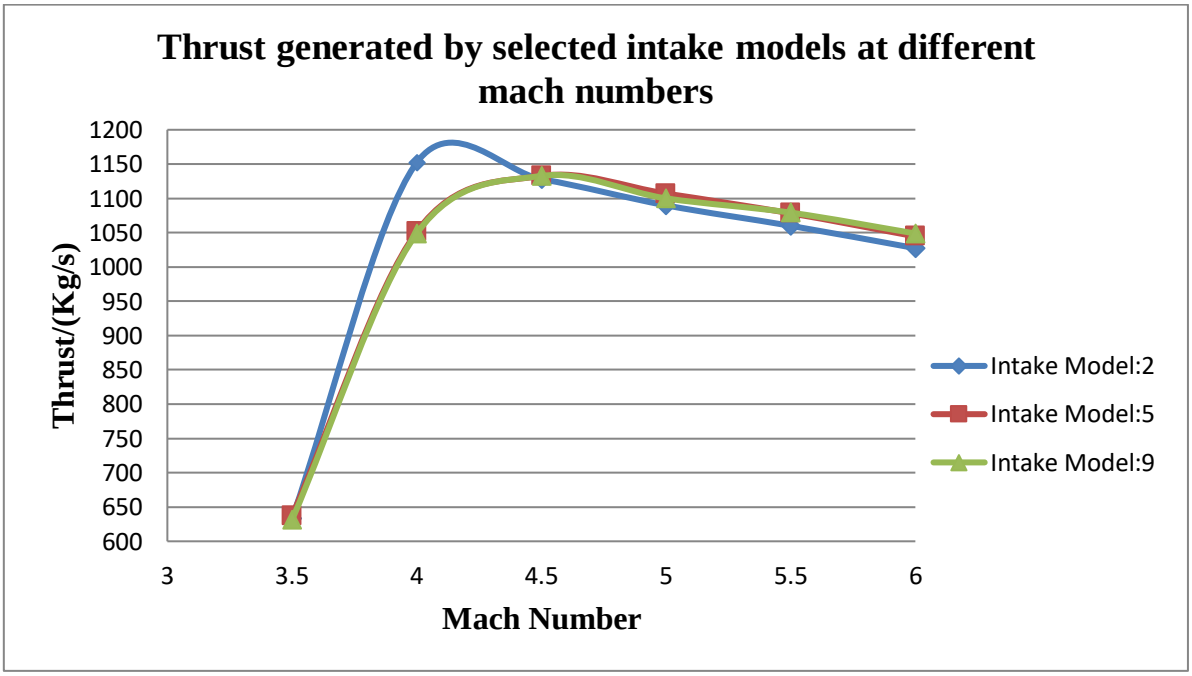

Fig.4.57: Thrust generated by selected intake models at different mach numbers.

ISSN No:-2456-2165

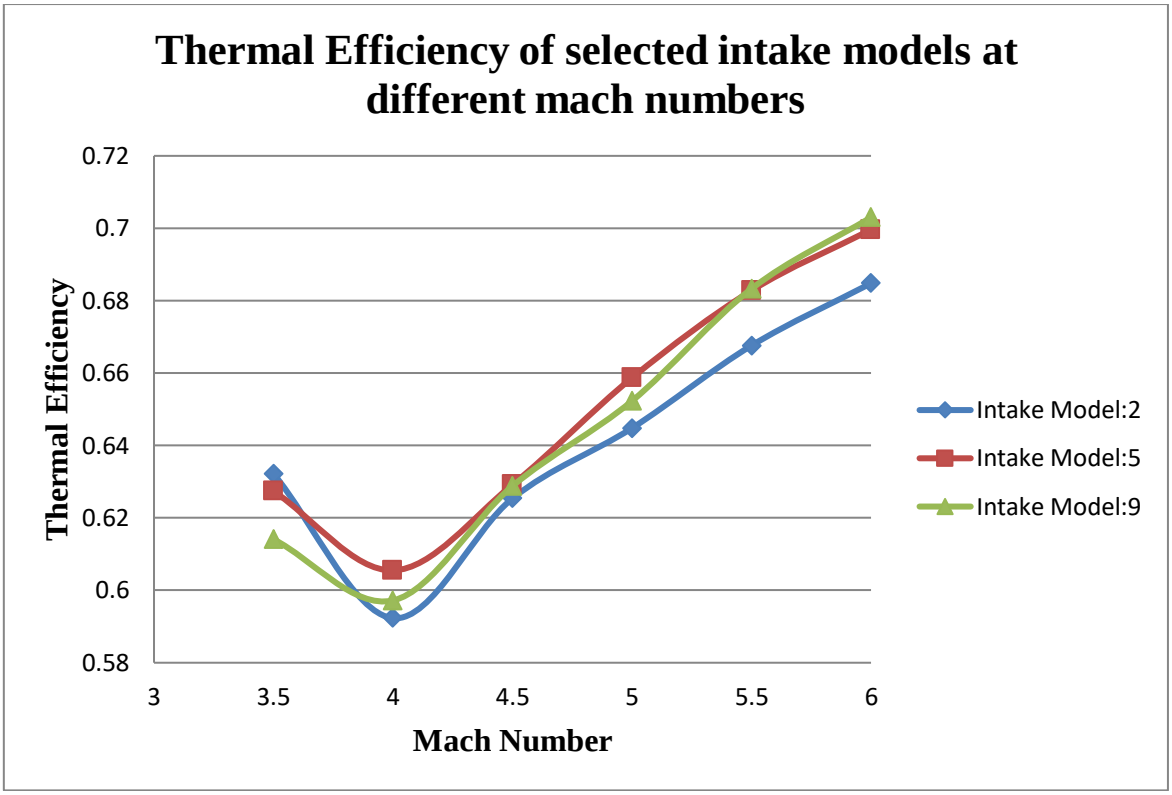

Fig.4.58: Thermal Efficiency of selected intake models at different mach numbers

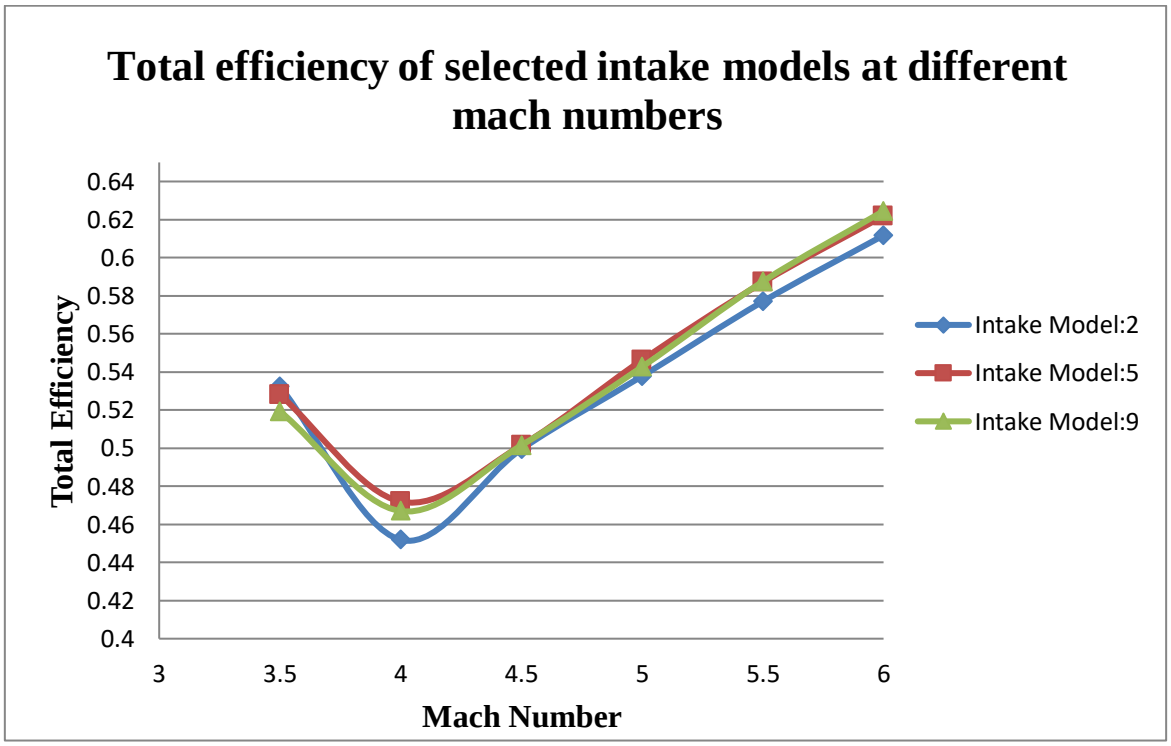

Fig.4.59: Total efficiency of selected intake models at different mach numbers

ISSN No:-2456-2165

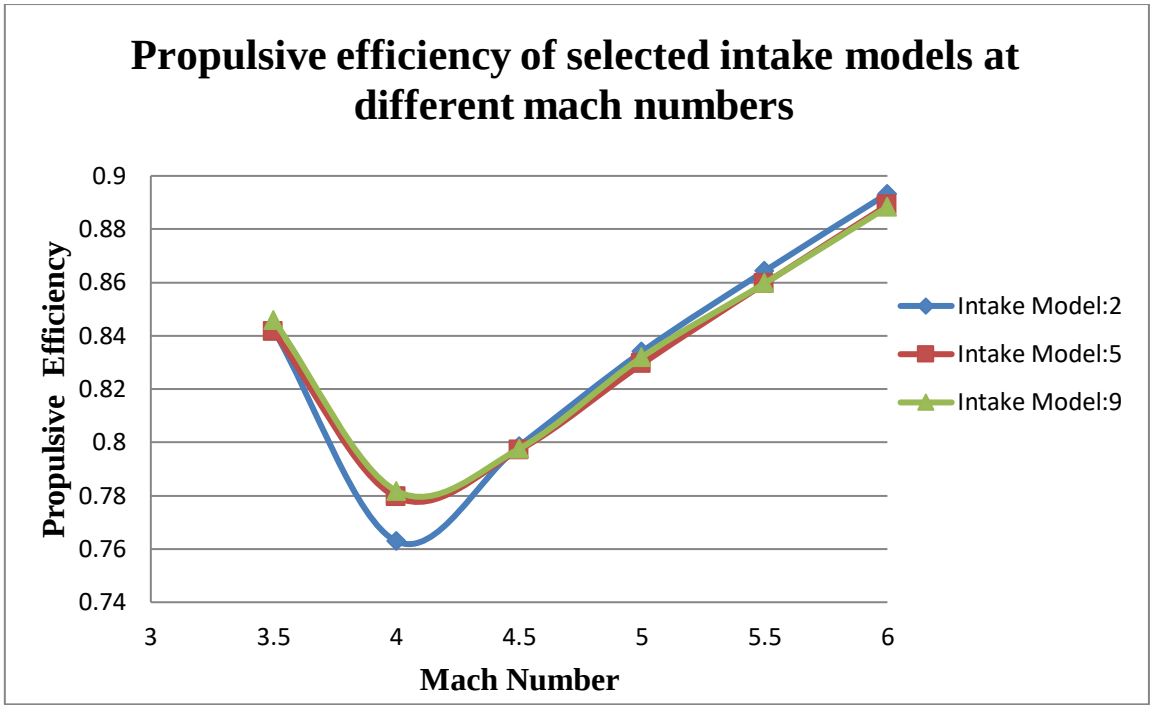

Fig.4.60: Propulsive efficiency of selected intake models at different mach numbers

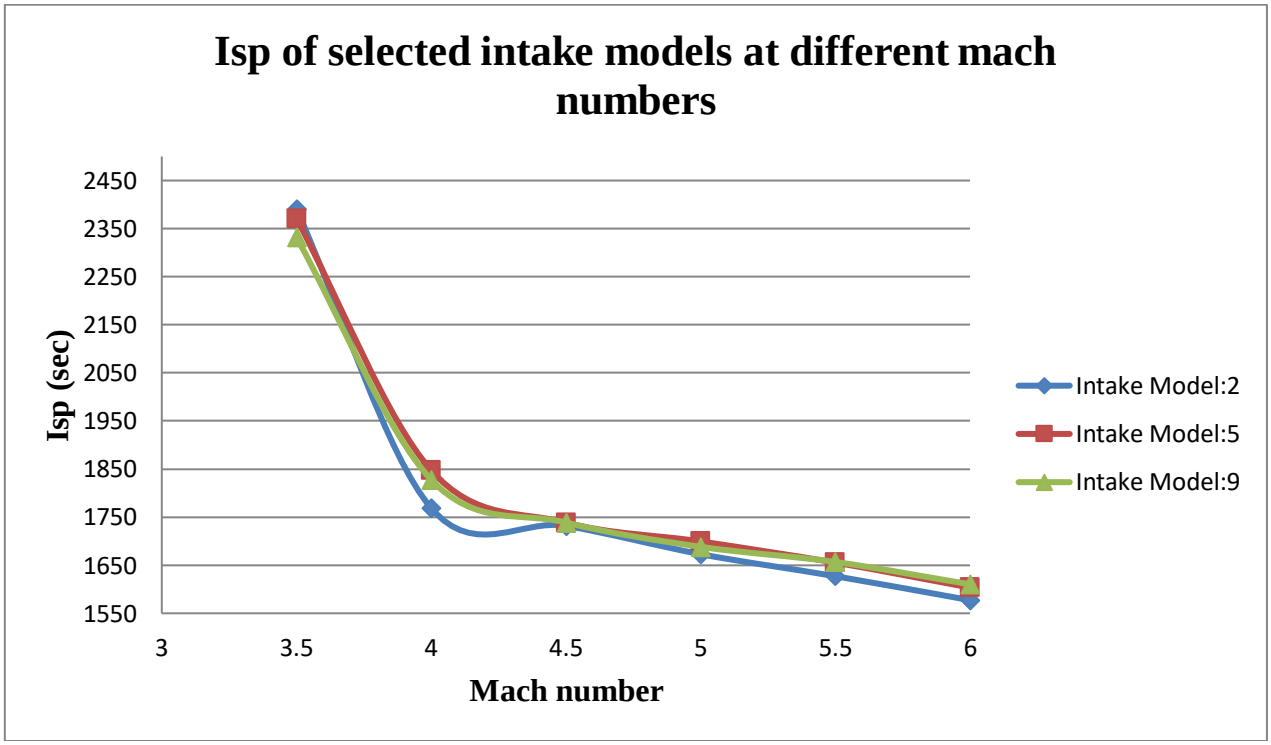

Fig.4.61: Isp of selected intake models at different mach numbers

V. CONCLUSION

From figures given in the previous section, for hypersonic intake geometry with no moving parts in a condition of lower starting Mach number, intake with 2 ramps has the highest performance in terms of thrust generation, Isp & efficiencies among three selected models at lower Mach number i.e. Mach 3.5 for our case of analysis and lowest performance at Mach number 6, while intake with four 4 has the highest performance in terms of thrust generation, Isp & efficiencies among three selected models at Mach number 6 and lowest performance at lower Mach number 3.5. The reason behind the performance degradation of 4 ramp intake at lower Mach number is the strong shock generation at the entrance of the isolator, which decreases pressure recovery up to a large extent. We have also seen that designing four ramp intakes for lower starting Mach numbers is very difficult as the intake unstart problem is predominant in this case. Intake with 3 ramps has a quite good performance at both lower and designed Mach

numbers. Even at Mach 6, intake with 3 ramps has performance very similar to intake with 4 ramps. So we can say that intake with 3 ramps is the best choice for lower starting Mach number condition. If we talk about fuel selection, then octane is suitable fuel when hypersonic intake with lower starting Mach number scenario is to be considered as it has a lower self-ignition temperature which plays a very important role in this type of scenario.

REFERENCES

[1]. Michael K. Smart, "Scramjet inlets," Centre for Hypersonics, TheUniversity of Queensland Brisbane 4071, Australia, September 2010.
[2]. Fry, Ronald S. "A Century of Ramjet Propulsion Technology Evolution,"Journal of Propulsion and Power. January-February 2004, Volume 20, No. 1, pp.27-58 doi:10.2514/1.9178
[3]. Anderson, John D., Jr., "Fundamentals of Aerodynamics," 5thEdition, the McGraw-Hill Companies, Inc, New York, 2011
[4]. Luu Hong Quan, Nguyen Phu Hung, Le Doan Quang, Vu Ngoc Long,"Analysis and Design of a Scramjet Engine Inlet Operating from Mach 5 to Mach 10,"*International Journal of Mechanical Engineering and Applications.* 2016, Vol. 4, No. 1, pp. 11-23 doi: 10.11648/j.ijmea.20160401.12
[5]. Augusto F. Moura, Maurício A. P. Rosa, "A Numerical Investigation of Scramjet Engine Air Intakes for the 14-X Hypersonic Vehicle"
[6]. Atulya Sethi, "Design and Analysis of Scramjet Inlet," *International Journal of Engineering Inventions.* August, 2018,Vol. 7, Issue 8, pp. 50-59
[7]. Murugesan S, Dilip A Shah, Nirmalkumar D, "Computational Analysis of Scramjet Inlet," *International Journal of Recent Scientific Research.* April, 2015, Vol. 6, Issue 4, pp.3391- 3403
[8]. Azam CheIdris, Mohd Rashdan Saad, Hossein Zare-Behtash, Konstantinos Kontis, "Luminescent Measurement Systems for the Investigation of a Scramjet Inlet-Isolator," 9 April 2014, Vol. 4, pp. 6606-6632 doi:**https://doi.org/10.3390/s140406606**
[9]. Curran, E.T., and S.N.B. Murthy, "Scramjet Propulsion," American Institute of Aeronautics and Astronautics. 2000, Vol. 189: Progress in Astronautics and Aeronautic.
[10]. Devendra Sen, Apostolos Pesyridis, and Andrew Lenton, "A Scramjet Compression System For Air Transportation Vehicle Combined Cycle Engines," Energies. 2018, Vol. 11, Issue 6 doi:**https://doi.org/10.3390/en11061568**
[11]. Qi-Fan Zhang, Hui-Jun Tan, Hao Chen, Yong-Qing Yuan, and Yu-Chao Zhang, " Unstart Process of a Rectangular Hypersonic Inlet at Different Mach Number," American Institute of Aeronautics and Astronautics. 2016, Vol. 54, No. 12, pp. 3681-3691doi::10.2514/1.J055005
[12]. Heiser, William H., David T. Pratt, Daniel H. Daley, and Unmeel B. Mehta, "Hypersonic Airbreathing Propulsion," American Institute of Aeronautics and Astronautics. Washington, D.C., 1994.
[13]. Handbook of Chemistry and Physics, 88th Edition, 2007 – 2008, CRC Press, LLC, URL: http://www.hbcpnetbase.com/; Section 2: Definitions of Scientific Terms; Section 16: Flammability of Chemical Substances.
[14]. Handbook of Aviation Fuel Properties, CRC Report No. 635, 3rd edition, Coordinating Research Council, Inc (CRC), Alpharetta, GA, 2004
[15]. Kuchta, J. M., "Investigation of Fire and Explosion Accidents in the Chemical, Mining, and Fuel-Related Industries" – a Manual, Bulletin 680, U.S. Bureau of Mines, 1985, Appendix A.
[16]. Edwards, Tim. " 'Kerosene' Fuels for Aerospace Propulsion – Composition and Properties," 38th AIAA/ASME/SAE/ASEE Joint Propulsion Conference & Exhibit. 7 July 2002, Indianapolis, Indiana. AIAA Paper 2002-3874 doi:https://doi.org/10.2514/6.2002-3874
[17]. Ciccarelli, G., and J. Card. "Detonation in Mixtures of JP-10 Vapor and Air," AIAA Journal. February 2006,Volume 44, No. 2. doi:https://doi.org/10.2514/1.18582
[18]. Kristen N. Roberts, Analysis and Design of a hypersonic Scramjet engine with a starting Mach number of 4.00, Master's thesis, The University of Texas at Arlington, August 2008.